https://doi.org/10.5194/egusphere-2023-471
Preprint. Discussion started: 27 March 2023

Sub-frontal niches of plankton communities driven by transport and trophic interactions at ocean fronts

Inès Mangolte[1], Marina Lévy[1], Clément Haëck[1], and Mark D. Ohman[2]

[1]Sorbonne Université, Laboratoire d'Océanographie et du Climat, Institut Pierre Simon Laplace (LOCEAN, SU/CNRS/IRD/MNHN), 75252 Paris Cedex 05, France
[2]Scripps Institution of Oceanography, University of California San Diego, La Jolla, California, 92093-0218 United States of America

Correspondence: Inès Mangolte (ines.mangolte@locean.ipsl.fr)

Abstract. Observations and theory have suggested that ocean fronts are ecological hotspots, associated with higher diversity and biomass across many trophic levels. The hypothesis that these hotspots are driven by frontal nutrient injections is seemingly supported by the frequent observation of opportunistic diatoms at fronts, but the behavior of the rest of the plankton community is largely unknown. Here we investigate the organization of planktonic communities across fronts by analyzing 8 high resolution transects in the California Current Ecosystem containing extensive data for 24 groups of bacteria, phytoplankton and zooplankton. We find that a distinct frontal plankton community characterized by enhanced biomass of not only diatoms and copepods but many other groups of plankton such as chaetognaths, rhizarians and appendicularians emerges over most fronts. Importantly, we find spatial variability at a finer scale (typically 1-5 km) than the width of the front itself (typically 10-30 km) with peaks of different plankton taxa at different locations across the width of a front. Our results suggest that multiple processes, including horizontal stirring and biotic interactions, are responsible for creating this fine-scale patchiness.

1 Introduction

Ocean fronts are narrow regions of elevated physical gradients that separate water parcels with different properties. Some fronts are simply boundaries between biogeographical domains with distinct biological communities (Mousing et al., 2016; Tzortzis et al., 2021; Haberlin et al., 2019) that can overlap and mix in the frontal region (Lévy et al., 2014; Clayton et al., 2014). But many empirical and modelling studies have also pointed out that fronts can be specific "biological hotspots", attractive to higher predators (Belkin, 2021; Prants, 2022) and often associated with an enhanced local productivity of diatoms (Allen et al., 2005; Ribalet et al., 2010; Taylor et al., 2012; Lévy et al., 2015). Theory has shown that frontogenesis, i.e. the intensification of a surface density gradient, leads to the vertical injection of nutrients into the euphotic zone (Klein and Lapeyre, 2009; Lévy et al., 2012; Mahadevan, 2016). Although this frontal supply of nutrients is generally assumed to propagate up the trophic web, the mechanistic link between nutrient supply and higher trophic levels is still very poorly understood, in large part because of the limited information on the intermediate trophic levels. Some studies have shown that the biomass and the activity of copepods is stimulated over fronts (Thibault et al., 1994; Ashjian et al., 2001; Ohman et al., 2012; Derisio et al., 2014) and that mesozooplankton acoustic backscatter (Powell and Ohman, 2015) and gelatinous zooplankton can aggregate

https://doi.org/10.5194/egusphere-2023-471
Preprint. Discussion started: 27 March 2023

at fronts (Graham et al., 2001; Luo et al., 2014). In addition, modelling studies suggest that the increased nutrient supply can create complex competitive interactions among phytoplankton groups over fronts (Lévy et al., 2014, 2015; Mangolte et al., 2022). Finally, fronts are associated with extremely dynamic horizontal currents that can transport water and their associated plankton communities over large distances (Clayton et al., 2013, 2017; de Verneil et al., 2019). In line with these different mecanisms, Lévy et al. (2018) proposed a rationalisation of the biological impact of fronts, distinguishing between between active (increased production in response to the nutrient injections), passive (stirring by horizontal currents) and reactive (biotic interactions) processes.

Here, we test the hypothesis that plankton communities at fronts are primarily shaped by the bottom-up transmission of the effect of the nutrient injections ("active processes"). To that end, we evaluate whether the taxonomic and spatial structure of the entire planktonic community (from bacteria to zooplankton) are consistent with a bottom-up response to nutrient injections. We then show that other processes, such as horizontal transport and trophic interactions ("passive" and "reactive" processes) also contribute to the structure of frontal communities, leading to plankton niches at a sub-frontal scale. More specifically, we address the following questions :

1. Are fronts commonly associated with a biological enhancement ("peak fronts") or are they simply a boundary between two biologically distinct environments ("transition fronts") ?

2. In the case of peak fronts, are there changes in community structure associated with biomass enhancement ? Do all species benefit from the frontal dynamics or are there winners and losers ?

3. What is the spatial organization of the plankton community across a front ? Is there biological variability at a scale finer than the physical scale across the front ?

To answer these questions, we performed a meta-analysis of in-situ data collected as part of the CCE-LTER (*California Current Ecosystem* Long Term Ecological Reasearch) program during four cruises between 2008 and 2017 (Fig. 1 and Tab. 1). The CCE is an eastern boundary upwelling system with a strong regional cross-shore gradient from colder waters inshore to warmer waters offshore. This regional gradient is constantly stirred by the mesoscale horizontal circulation, which results in a multitude of small-scale density fronts (Mauzole et al., 2020). The CCE region is populated both by mesoscale eddies (Chelton et al., 2011), usually propagating westward, detectable from their SSH anomaly and associated with geostrophic currents, and by coastal filaments originating from the coast and containing recently upwelled water parcels moving offshore through a combination of geostrophy and Ekman transport (Chabert et al., 2021). These two types of structures interact and lead to a complex interleaving of water masses separated by different types of frontal features forced by different processes (Renault et al., 2021; Mauzole et al., 2020). The empirical measurements include the quantification of the biomass of 24 taxa in the planktonic community, from heterotrophic and bacteria to phytoplankton and mesozooplankton (Fig. 3). The data were collected along eight high resolution transects (with a spacing of 1 to 5 km between stations) conducted across various structures, including upwelling filaments and geostrophic fronts; we identified ten separate fronts from gradients in thermodynamical properties (density, temperature, salinity), as two transects crossed filaments with fronts on either side.

https://doi.org/10.5194/egusphere-2023-471
Preprint. Discussion started: 27 March 2023

We first investigate whether the various groups of plankton have enhanced biomass over fronts compared to the fronts' immediate surroundings (the "background"). We find that over most fronts, there is a specific frontal plankton community characterized by biomass maxima of diatoms and many zooplankton taxa, but also minima of other phytoplankton taxa, particularly cyanobacteria. Then, we examine the fine scale spatial organization of the planktonic community by describing the width and the position along the transect of these biomass peaks relative to the width of the density gradient. We find that, contrary to expectations from the theoretical structure of vertical circulation at fronts (Klein and Lapeyre, 2009), the biomass peaks are not aligned with the density gradient and their locations show an unexpectedly high level of variability among taxa.

2 Methods

We used data collected during four cruises of the California Current Ecosystem Long Term Ecological Research (CCE-LTER, Ohman et al. (2013)) program (Table 1). During each cruise, one to three transects were conducted across frontal structures (Fig. 1. Physical, chemical and biological properties were measured at nine to twelve stations regularly spaced at high resolution along the transects and were all performed in a single night (Fig. 2). At each station, 24 different plankton taxa were identified using measurements made using a CTD-rosette for bacteria and phytoplankton and a net tow for zooplankton (Fig. 3). Other measurements included the Chl-a fluorescence and the concentration of nutrients. Importantly, the same observations and methodology were applied for all CCE-LTER transect cruises, which provides a consistent data set, although the data were collected in different years. Our method relies on the comparison between the plankton community over the fronts and the community in the immediate surrounding of the fronts. Moreover, we also examine the fine-scale organisation of the plankton community across the front. The first step in our analysis is thus the identification of the stations that we identify as front stations, and we compare the community structure at these stations with the community structure in the neighbouring background stations.

2.1 Data

At each station, a CTD vertical profile was conducted down to $100\mathrm{m}$ and water samples were collected in Niskin bottles at discrete depths on the ascent; zooplankton samples were then collected with a 202 $\mu\mathrm{m}$ mesh vertical Bongo net tow (also from 0 to $100\mathrm{m}$). In addition to the temperature and salinity recorded by the CTD, a fluorometer measured the in-vivo chlorophyll-a fluorescence along each vertical profile. The concentration of nutrients (nitrate, phosphate, silicic acid, nitrite and ammonium) was determined at discrete depths from the Niskin bottle samples. The plankton samples were later analyzed on land using three different methods (Fig. 3):

- Flow cytometry was performed on the Niskin bottle water samples (0-$100\mathrm{m}$), producing the abundance ($\mathrm{number\ of\ cells/L}$) of 4 taxa of pico-plankton ($< 2\ \mu\mathrm{m}$) identified by their light-scattering properties.
- HPLC (High Performance Liquid Chromatography) was performed on all the Niskin bottles (0-100m) during the first cruise (A-front) and on the surface Niskin bottle only for the other 3 cruises (E-front, C-front and F-front). The concen-

https://doi.org/10.5194/egusphere-2023-471
Preprint. Discussion started: 27 March 2023

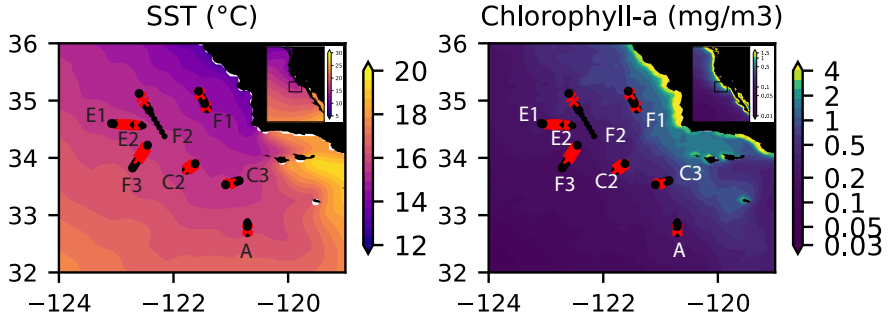

Figure 1. Location of the transects sampled by the CCE-LTER program in summer and autumn between 2008 and 2017. Transect names (A, C2, C3, E1, E1, F1, F2, F3) are indicated close to the first station of their corresponding transect (note that the stations of E1 and E2 are in the same location, with E1 starting on the West and E2 on the east); stations identified as frontal stations are indicated by red crosses and stations identified as background stations by black circles. Transects E2 and F1 each contain 2 fronts, leading to a total of 10 fronts for the 8 transects. Background color : July climatology over the study period (2008-2017) of (a) SST and (b) chlorophyll-a

Table 1. Name and characteristics of the eight CCE-LTER transects. C1 was aborted and is not included in this study.

Cruise Number	Structure Name	Transects	Date	Length	Number of stations	Resolution	References
P0810	A-front	A	24-25 Oct 2008	25 km	9	2.8 km	Landry et al. (2012) and references therein
P1106	C-front («California Current front»)	C1	19-20 June 2011	6 km	5	1.3 km	Krause et al. (2015) Brzezinski et al. (2015)
		C2	2-3 July 2011	20 km	10	1.9 km	
		C3	15-16 July 2011	25 km	10	2.3 km	
P1208	E-front («Eddy front»)	E1	4-5 August 2012	50 km	13	2-5 km	Bednaršek and Ohman (2015) Stukel et al. (2017) de Verneil et al. (2019)
		E2	20-21 August 2012	50 km	10	4.9 km	
P1706	F-front («Filament front»)	F1	7-8 June 2017	35 km	11	3.4 km	Zaba et al. (2021)
		F2	17-18 June 2017	90 km	11	8.4 km	
		F3	22-23 June 2017	50 km	11	4.6 km	

trations of chlorophyll-a and accessory pigments were measured and used to determine the contributions (percentage) of 8 phytoplankton taxa relative to the total chlorophyll (Goericke and Montoya, 1998).

– Zooplankton samples were collected using vertical Bongo nets (0.71m diameter, mesh size of 202µm) retrieved from 100 m, preserved in 1.8% buffered formaldehyde and the organisms then identified in the lab using the ZooScan semi-

https://doi.org/10.5194/egusphere-2023-471
Preprint. Discussion started: 27 March 2023

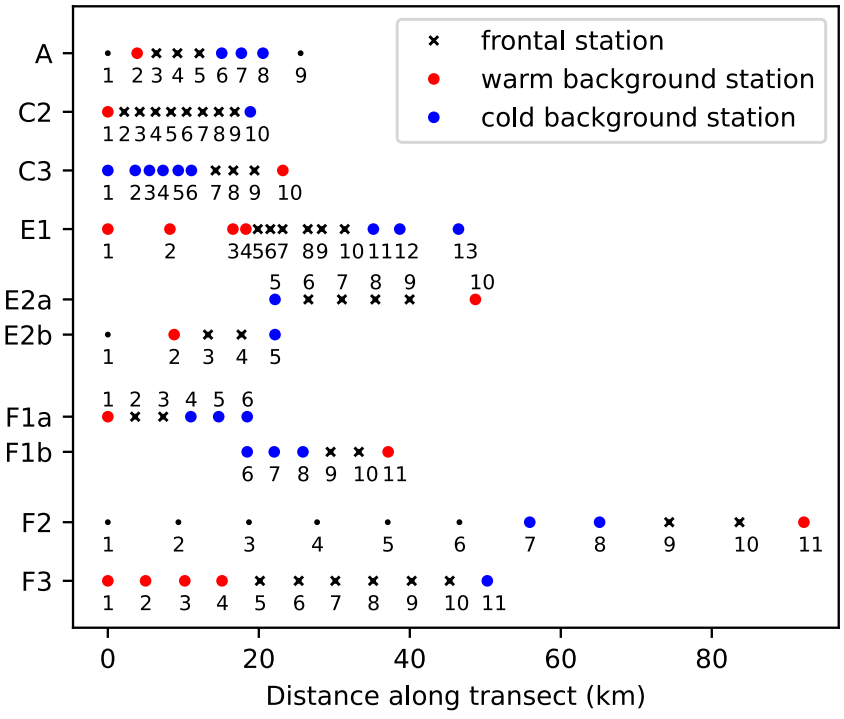

Figure 2. Number of stations and spacing between stations along each of the eight CCE-LTER transects. Stations are classified into frontal stations (black crosses), and background stations on the warm side of the front (red dots) or cold side of the front (blue dots) (see text). Note that transects E2 and F1 contain two fronts and are shown twice (E2a/E2b, F1a/F1b), once for each front, with empty circles over the second front.

automated imaging system (Gorsky et al., 2010; Ohman et al., 2012) with 100% manual validation. The analysis produced the vertically integrated abundance (number of organisms/m^2) of 15 groups of meso-zooplankton.The abundances of eggs (mainly belonging to copepods and euphausiids) and nauplii (the juvenile form of copepods and other crustaceans) were also determined; the ratios of eggs or nauplii to adults is used as a proxy of secondary production.

The 24 individual taxa were then grouped into 7 functional groups. The functional groups were defined on the basis of their ecological and biogeochemical roles rather than size and taxonomy. For instance, diatoms were separated from the other eukaryotic phytoplankton because of their high potential for growth under nutrient replete conditions, while rhizaria and tunicates were included in the pico-grazers group because they all consume bacteria despite the former being protists and the latter metazoans. Since the different instruments provide measurements in different units, the abundances of the taxa were first converted into carbon biomass which served as the common currency, and summed to obtain the total for each group. Appropriate conversion factors were chosen according to the litterature, and include carbon content per cell for flow cytometry (Garrison et al., 2000), chlorophyll:carbon ratios for HPLC (Li et al., 2010) and carbon per organism values for ZooScan (Lavaniegos

https://doi.org/10.5194/egusphere-2023-471
Preprint. Discussion started: 27 March 2023

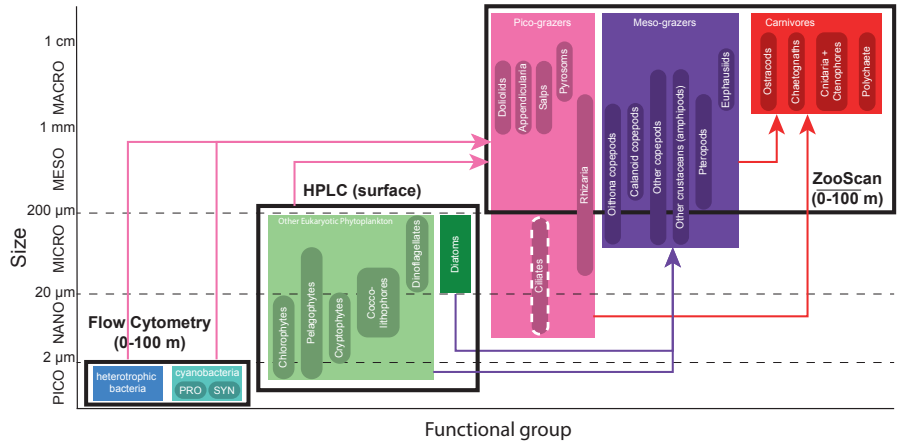

Figure 3. The 24 plankton taxa measured as part of the CCE-LTER program, sorted by size class (y-axis) and trophic group (color). Shown are the different instruments used to measure their abundance (black rectangles). Arrows represent the main predatory interactions between groups: pico-grazers consume bacteria and phytoplankton, meso-grazers consume eukaryotic phytoplankton, and carnivores consume grazers. Flow cytometry produces the abundance of heterotrophic and cyano-bacteria collected in Niskin bottles at discrete depths (about 7 levels from 0-100m). HPLC produces the concentration of 6 taxa of eukaryotic phytoplankton collected in Niskin bottles at discrete depths for the A-front and at the surface only for the other cruises. ZooScan produces the vertically integrated abundance (0-100m) of 15 taxa of zooplankton collected with a Bongo net tow. Nano and microzooplankton (such as ciliates) were only sampled in the A-front cruise (using epifluorescence microscopy) and are not part of this meta-analysis.

and Ohman, 2007). The vertically resolved data derived from Niskin bottles (flow cytometry for all the transects and HPLC for the A-front) were then vertically averaged. Thus all the data are expressed as a carbon concentration ($\mu\mathrm{gC}/\mathrm{m}^3$).

It should be noted that nano- and micro-zooplankton (which mainly consists of heterotrophic protists such as nanoflagellates and ciliates) were also measured during the A-front cruise using epifluorescence microscopy (Taylor et al., 2012). However, they were not sampled during the subsequent cruises and thus are not included in this meta-analysis. Cyanobacteria (PRO and SYN) were measured by both flow cytometry and HPLC; flow cytometry data were depth resolved in all transects while the HPLC data were only depth resolved in the A-front transect (the other transects only include the surface value). There are some quantitative differences between the data produced by the two methods, but the patterns are generally similar (Supp. Fig. A6 and A7). In the following analysis, we use the flow cytometry data since they are vertically resolved. Finally, pico-eukaryotes (measured with flow cytometry) were not incorporated in our analysis because they include photosynthetic and heterotrophic organisms that belong to different functional groups. The photosynthetic pico-eukaryotes were however measured independently by HPLC. Moreover, because the category includes a vast variety of organisms with a wide range of carbon content values, they could not be robustly converted to carbon biomass.

https://doi.org/10.5194/egusphere-2023-471
Preprint. Discussion started: 27 March 2023

2.2 Identification of fronts

During the CCE-LTER cruises, fronts were first roughly identified using real-time satellite data of Sea Surface Temperature (SST) and Sea Surface Height (SSH) and their location and physical structure more precisely localized with a free-fall Moving Vessel Profiler (MVP, Ohman et al. (2012)). This permitted the transects to be successfully positioned in the cross-frontal direction. All transects show distinct density and/or temperature and salinity gradients, indicating the presence of a front (uppermost panels in Fig. 4). Each front is sampled by at least one station and in most cases at least three. Two of the transects (E2 and F1) crossed a cold filament and thus included two fronts, each corresponding to one boundary of the filament. These two transects were separated in two half-transects prior to analysis at the center of the filament (stations 5 in transect E2 and stations 6 in transect F1, indicated by vertical lines in Fig. 4). This led to a total of ten segments, each containing one front (Fig. 2).

Along each segment, we sorted the stations into those belonging to fronts (black crosses in Fig. 2 and Fig. 4) and those in the background, separating the cold side and warm side of the front (blue and red circles in Fig. 2, respectively). This was done on the basis of the along-transect gradients of density, temperature and salinity, averaged between the surface and $50\mathrm{m}$. Gradients were computed using central differences except at the boundaries where one-side differences were used. The distributions of density, temperature and salinity and of their gradients along the transects showed a variety of situations: the sign and intensity of the density gradients strongly varied among transects, as well as their structure (Fig. 4 and supp. Fig. A9); some fronts were clearly associated with a marked density gradients (i.e., A, E1), another was compensated i.e., there was no significant density gradient but there were marked temperature and salinity gradients (i.e., C2), others consisted of density steps (i.e., F3).

To sort the stations, we used the absolute values of the gradients and we normalized them by their averaged value along the transect (hereafter $\Delta\rho$, ΔT and ΔS are the normalized gradients and they are equal to one when the gradient is equal to the mean gradient). In order to capture the variety of situations described above, we used the following criteria to identify frontal stations and background stations:

1. Stations where $\Delta\rho > 1$ or $\Delta T > 1$ or $\Delta S > 1$ were classified as a front, unless they were at the edge of a transect.

2. Some stations have relative gradients lower than 1 but are located between front stations; these stations constitute steps of a larger frontal structure and are also classified as frontal stations. This was the case for stations 5-6 of transect C2 and station 8 of transect F3.

3. Isolated stations with strong gradients outside of the targeted frontal area were excluded from the analysis (meaning they are neither front nor backgound) when they were part of a separate physical structure. This was the case for stations 9 of transect A and station 1 of E2b where density variations reflect the large-scale cross-shore gradient; for station 1 of transect A which is located at the edge of the California Current, with a salinity gradient of opposite sign from the main front; and for stations 1-6 of transect F2 which are part of another filament (Supplementary text).

https://doi.org/10.5194/egusphere-2023-471
Preprint. Discussion started: 27 March 2023

4. Stations where $\Delta\rho > 1$ or $\Delta T > 1$ or $\Delta S > 1$ located at the edge of a transect where classified as background in order to provide at least one point of comparison with the other front stations of the transect. This was the case for station 11 of transect F3, station 1 of half-transect F1a, station 5 of half-transect E2b and station 1 of transect C2.

5. All remaining stations where classified as background.

Within background stations, we then identified those located on the cold (resp. warm) side of each front. Finally, we identified the central position of the front (in km) and the width of the front, defined as the number of front stations multiplied by the resolution of the transect (in km).

2.3 Front enhancement factor

We quantified the biological effect of each front by measuring a Front Enhancement Factor (FEF) for each plankton taxon, as well as for total phytoplankton biomass and Chl-a fluorescence. The front enhancement factor was computed when there was a biomass peak at the front, and was undefined otherwise. A peak at the front implied that the taxon has an extremum in biomass (maximum or minimum) at one of the front stations, relative to values on both sides of the front. We defined the front enhancement factor as the relative difference between the peak biomass at the front and the average biomass in the background stations surrounding the front:

$$FEF = \frac{F_{peak} - \bar{B}}{\bar{B}} * 100 \tag{1}$$

where F_{peak} is the biomass extremum among frontal stations (minimum or maximum) and $\bar{B}$ is the average biomass of the background stations (including cold side and warm side).

2.4 Identification of biomass peaks

Along each transect, taxa exhibited large changes in their biomass at the scale of a few stations, with clearly recognizable peaks (Fig. 4 and Supp. Fig. A11,A12 and A13). We detected these biomass peaks (minima or maxima) along each transect, their position (center of the peak) and their width. It is important to note that the biomass peak detection and the location of the physical fronts are made independantly from one another, the latter on the basis of the along-transect distribution of density, temperature and salinity, the first on the basis of the along transect distribution of the biomass of taxa. We compared the location of the biomass peaks with the location of the physical front. We measured the difference between their positions (in km), with the sign indicating whether the biomass peak is on the warm side of the front (positive values) or the cold side (negative values). Most biomass peaks were located over front stations, but some were outside of the fronts.

2.5 Regional context

Each front was placed in a larger regional context by using satellite data of Sea Surface Temperature (SST), Chlorophyll and Sea Surface Height (SSH) provided by the Copernicus Marine Environment Monitoring Service (https://marine.copernicus.eu/).

https://doi.org/10.5194/egusphere-2023-471
Preprint. Discussion started: 27 March 2023

We used the SST and Chlorophyll 4 km daily "cloud-free" (space-time interpolated) products distributed by OSTIA (https://doi.org/10.48670/moi-00165) and GlobColour (https://doi.org/10.48670/moi-00281), respectively. We used the SSH product (https://doi.org/10.48670/moi-00021) from the ERA global reanalysis at 8 km resolution.

We detected SST fronts by detecting large values of an Heterogeneity Index computed from SST data over windows of 20 km size (methods of Liu and Levine (2016); Haëck et al. (2023)). Stirring structures and regions of convergence were identified using backward in time Finite Size Lyapunov Exponents (FSLE) computed from horizontal velocities combining geostrophic currents derived from altimetry and Ekman currents derived from wind-stress data (Chabert et al., 2021). Water age, defined as the time elapsed since a parcel of water left the coast (defined as the 500 m isobath), was computed by advecting water parcels backwards until they reach the coast (Chabert et al., 2021). Snapshots of these satellite-based products at the time of each transect are shown in supp. Fig. A1 A2 A3 A4, and videos of their evolution over 6 months are available as digital supplementary material.

3 Results

In the next sections, we first describe the composition of the frontal community (i.e., the presence and intensity of biomass peaks at the front for the various plankton taxa using the enhancement factor) and then its spatial organization across the fronts (in terms of width of the peaks and position along the transect relative to the density gradient).

3.1 Biomass enhancement at fronts

3.1.1 Variabiliy between fronts

We find that while plankton communities are generally enhanced at fronts, this effect is not uniform across either the plankton groups or the fronts. In particular, front C3 represents an extreme case with no frontal enhancement of the total biomass and the majority of individual taxa. Such fronts are deemed "transition fronts" in contrast with the "peak fronts" that do have an enhanced frontal community with maxima of the total phyto- or zooplankton (Fig. 5).

We find that some trophic groups have more consistent behaviors than others : diatoms and pico-grazers are almost always strongly enhanced at every front, heterotrophic bacteria and other phytoplankton are generally weakly enhanced, while meso-grazers and carnivores are only occasionally strongly enhanced. However, the examination of these changes at a finer taxonomical resolution reveals that only a few of the taxa constituting these groups (such as diatoms, copepods, rhizarians, appendicularians, chaetognaths and polychaetes) are systematically enhanced. Most of the other zooplankton taxa have very intense peaks at only a few fronts (doliolids, euphausiids, pteropods, other crustaceans, cnidarians and ostracods), while the responses of the rest of the phytoplankton (diatoms excepted) tend to be more variable (alternatively increasing or decreasing depending on the front) and less intense.

https://doi.org/10.5194/egusphere-2023-471
Preprint. Discussion started: 27 March 2023

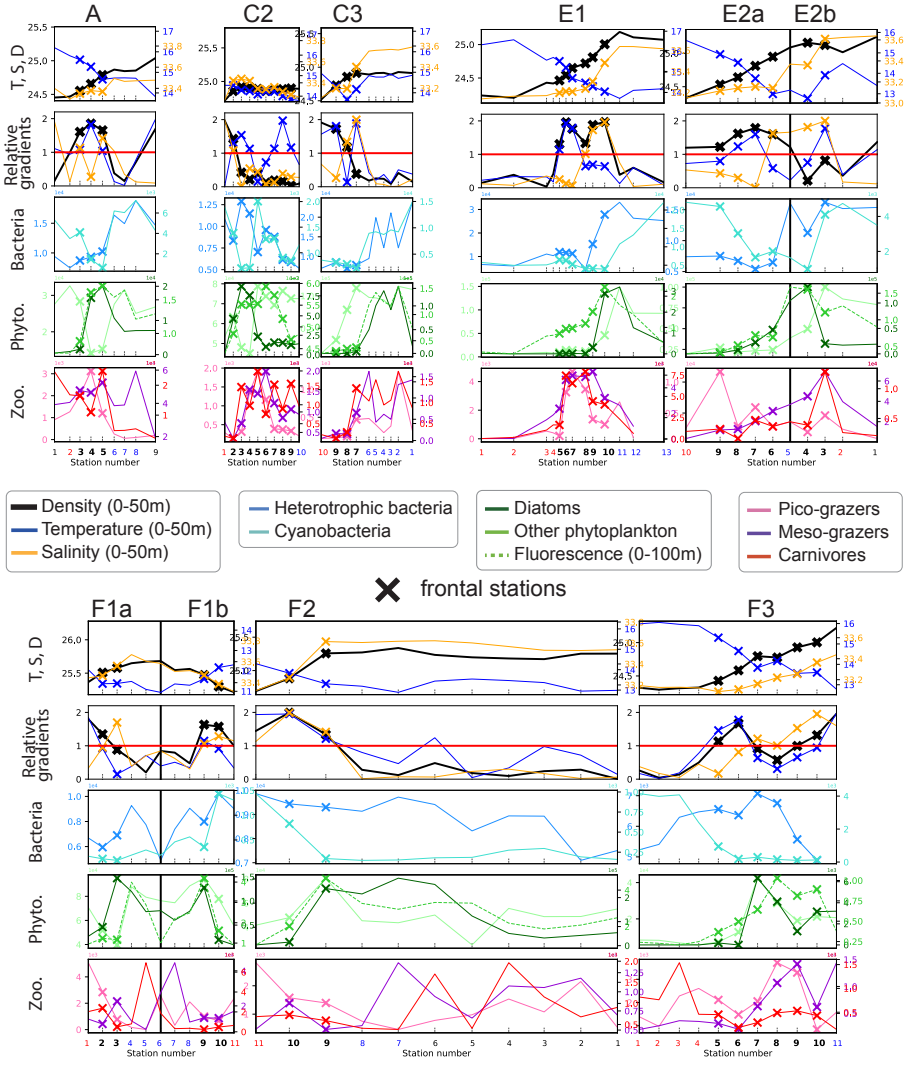

Figure 4. Distribution of density, temperature and salinity (first row), density, temperature and salinity relative gradients (second row), and the biomass of the seven plankton groups and fluorescence (third, fourth and fifth rows), along the 8 transects. Frontal stations are represented with crosses; and the station number is written at the bottom of each pannel in bold for frontal stations, red for warm background stations and blue for cold background stations. The center of the filaments in transects E2 and F1 is indicated with a black vertical line. The relative gradient threshold used to define frontal stations is indicated with a red horizontal line. The same scale is used along the x-axis for all transects. The same grid-spacing is used along the y-axis for density, temperature, salinity across all transects; and different scales are used for biomass.

https://doi.org/10.5194/egusphere-2023-471
Preprint. Discussion started: 27 March 2023

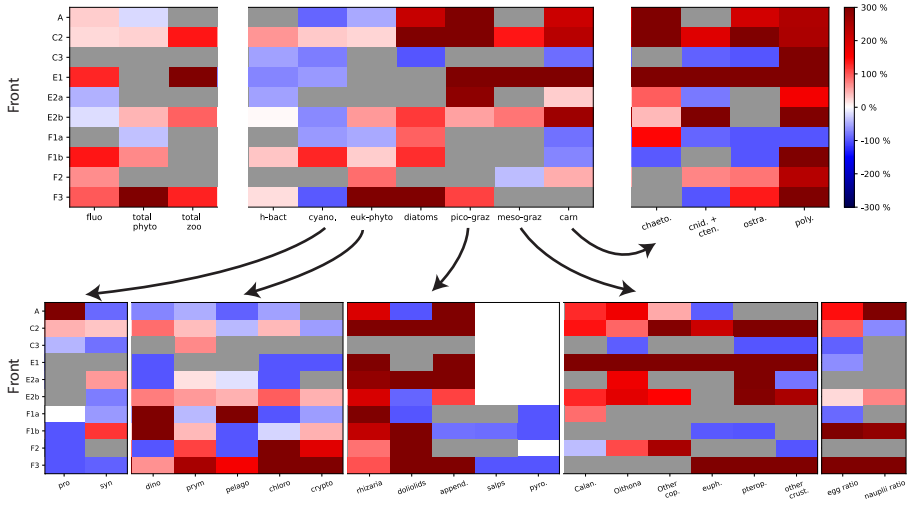

Figure 5. Front enhancement factor of the planton community for the 10 fronts sampled. Grey boxes indicate transition fronts: in such cases there is no enhancement at the front and the factor is undefined. Red and blue boxes indicate the intensity of the enhancement at the front: a species more abundant at the front than in the background is shown in red (positive enhancement factor); a species less abundant at the front than in the background is shown in blue (negative enhancement factor). The ten fronts are organized along the Y-axis, and the plankton along the x-axis. The first arraw shows the total biomass for phytoplankton, for zoolankton and the fluoresence. The second arraw shows the seven functional groups. The other arraws show each individual species constitutive of each group. The last arraw shows the early stages of copepods and auphausiid.

3.1.2 Modification of the taxonomic structure at peak fronts

At peak fronts, there is a maximum of either Chl-*a* fluorescence, or total phyto- or zooplankton biomass (Fig. 5, top left panel). However, the behavior of the individual trophic groups is not always that of the total, which implies that the signal of the total biomass can mask differences at finer taxonomical resolution. In some cases, the differences are simply in the intensity of the enhancement : for instance, at front C2 diatoms have a much stronger response than the other phytoplankton types. In other cases however, different groups can have completely diverging behaviors. For instance, at front E1, the enhancement of the total phytoplankton (visible in the fluorescence enhancement) masks a minimum of cyanobacteria, which represent less than 0.1% of the total biomass. At front A, the total zooplankton signal ("transition") is dominated by the most abundant group, the meso-grazers, whose "transition" masks the peaks of the pico-grazers and carnivores. But at front A, instead of one phytoplankton group dominating the total, the total is the balance of opposite tendencies of the various phytoplankton groups; Thus the maximum of diatoms and the minimum of the other phytoplankton results in a transition for the total.

At an even finer taxonomical resolution, the signal of a trophic group can also mask differences between the individual constituant taxa. This is particularly important because taxa belonging to the same trophic group have similar ecological roles and are expected to have similar responses to variations of their food supply. For instance, in the A-front, copepods and

https://doi.org/10.5194/egusphere-2023-471
Preprint. Discussion started: 27 March 2023

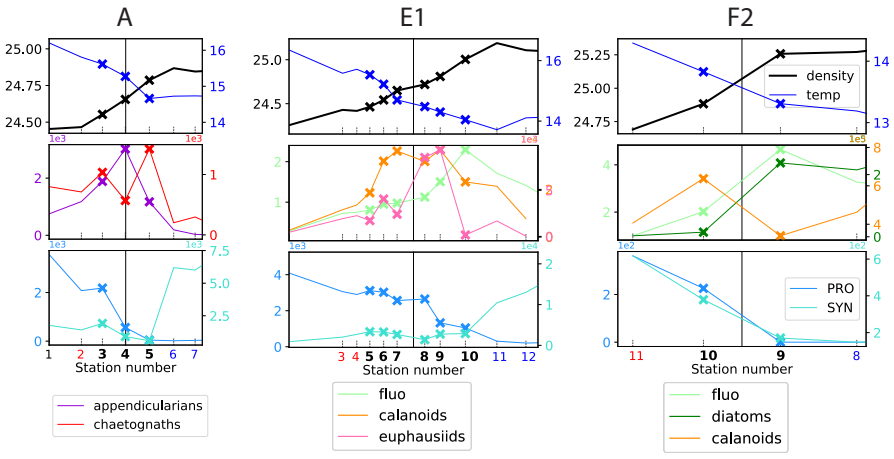

Figure 6. Distribution of physical and biological properties across three of fronts. The first row shows the physical structure of the fronts (temperature and density). The second row illustrates the fine scale spatial variability of the biomass peaks among two functionally different taxa (chaetognaths and appendicularians, front A), among functionally similar taxa (copepods and euphausiids, E1) and among prey and predator taxa (fronts E1 and F2). The third row illustrates the segregation of cyanobacteria on either side of the fronts ("transition"). Frontal stations are indicated by crosses; the stations on the warm and cold side are written in red and blue, respectively. The vertical line shows the middle of the frontal stations, defined with the density gradient. The same grid spacing is used for the x-axis of the three fronts.

220 euphausiids have a maximum and a minimum, respectively, despite the fact that both of them can consume diatoms (which also have a maximum).

3.2 Cross-frontal patchiness

In this section, we examine whether biomass peaks are aligned with the density gradient or shifted toward the warm or the cold side of the front. We investigate the variability across fronts and across plankton taxa : are the peaks of all taxa aligned with 225 the density gradient peak ? Does a single taxon have peaks with similar characteristics for all the fronts ?

Examination of the data along all high-resolution transects reveals that there is variability at a very fine scale (up to 1-2 km), i.e., between consecutive stations : biomass peaks of different taxa frequently occur at different stations, on different sides of the front and have differents widths (figure 6 and suppl. Figs A11,A12 and A13). Importantly, these different patterns among taxa concern taxa with a variety of ecological relationships, including prey/predator, competitors (i.e., taxa with similar 230 ecological roles belonging to the same functional group), and taxa with no direct interaction. These three cases are illustrated in figure 6 with diatoms/copepods and diatoms/euphausiids for the prey/predators (fronts E1 and F2, middle and right panel), copepods/euphausiids (both meso-grazers that consume large phytoplankton) for the competitors (front E1, middle panel) and appendicularians/chaetognaths for the taxa with little direct interaction (front A, left panel). In all of the cases, the peaks differ in location and widths.

https://doi.org/10.5194/egusphere-2023-471
Preprint. Discussion started: 27 March 2023

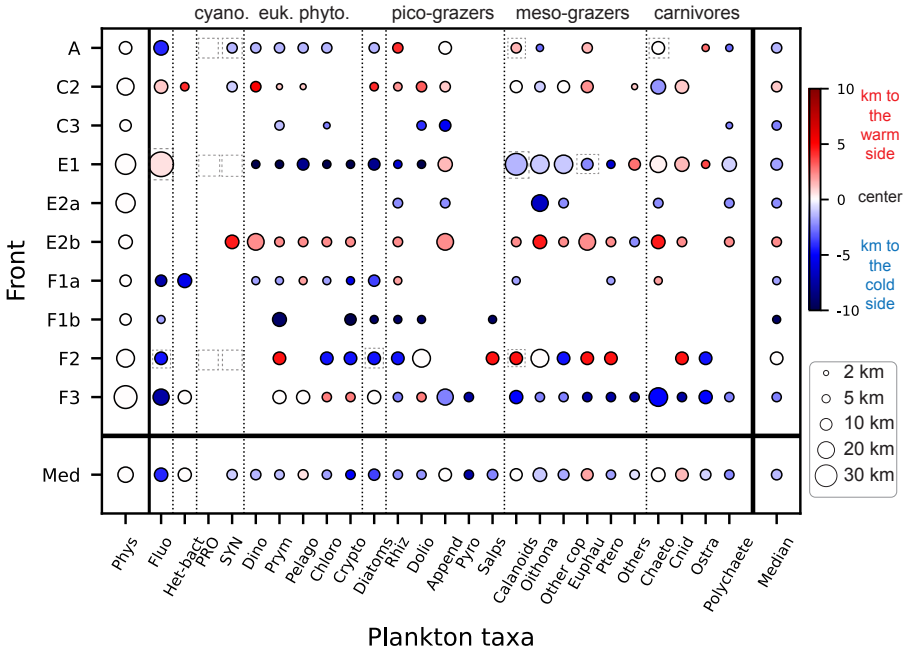

Figure 7. Size of the plankton biomass peaks, relative to the size of the front in the cross-front direction. The colorscale indicates the position of the biomass peaks relative to the center of the physical gradients (km) : positive values (red) mean that the biomass peak is shifted toward the warm side of the front and negative values (blue) mean that the biomass peak is shifted toward the cold side of the front. The size of the circle indicates the width of the peaks. The absence of a circle indicates the lack of a biomass peak ("transition" behavior). Dashed squares highlight the taxa presented in detail in fig. 6

Figure 7 compares the position and width of the biomass peaks and density gradients for each front and each taxon. We find that wide physical fronts (such as E1 and F3) can be associated with both narrow and wide biomass peaks while narrow fronts (such as A and C2) tend to be associated with narrow biomass peaks. Importantly, the physical scale of the front (width of the density gradient peak) is always wider than the biological scale of the fronts (width of the biomass peaks). The position of the biomass peaks is highly variable depending on the front. Over most fronts, plankton taxa are shifted toward the cold side (fronts A, E1, F1a, F1b), but over front (C2) they are shifted toward the warm side, and in two cases (F2 and F3) taxa are evenly split between the warm and cold side; plankton taxa are aligned with the density gradient in only one fronts, E2b, which is a narrow front with only one station for both the density and biomass peaks. Furthermore, individual taxa do not have systematic behaviors; they can peak on the warm or cold side, and have large or narrow peaks, depending on the front.

It should also be noted that some biomass peaks are shifted so far from the density gradient peak that they are located among the background stations. These peaks (such as the diatom peak in front E1 or the fluorescence peak in front F1a) were thus missed entirely in the computation of the peak enhancement factor.

https://doi.org/10.5194/egusphere-2023-471
Preprint. Discussion started: 27 March 2023

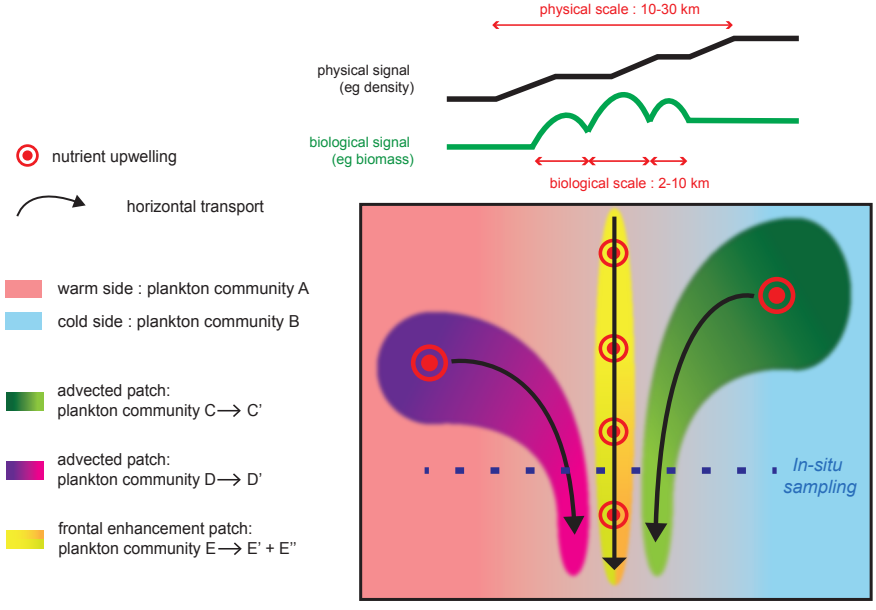

Figure 8. Schematic representation of the processes driving changes in community structure and fine scale cross-frontal patchiness at fronts. Black and green lines on top of the figure show the cross-front distributions of density and biomass; the physical signature is generally wider than the biological peaks, although the density or temperature gradients can increase in small steps. The green and purple plankton community mature as they are transported horizontal currents and converge at the front. Nutrient injections at the front stimulate plankton growth; the different conditions experienced by plankton (nutrient supply, light, temperature, biotic interactions) can create different communities toward the warm (yellow to green gradient) or cold side (yellow to orange gradient).

4 Discussion

4.1 How common are biomass enhancements at fronts ?

We find that seven out of the ten fronts included in this meta-analysis are associated with an enhanced biomass of phyto-
250 plankton and zooplankton, showing that fronts are generally more than simple barriers between plankton communities, and often support a specific frontal plankton community. This is consistent with a glider study of 154 fronts in the CCE-LTER region where Powell and Ohman (2015) found frequent front-related enhancement of Chl-a and mesozooplankton acoustic backscatter. However, it is possible that these "peak fronts" are over-represented in this dataset because the cruises specifically targeted intense and stable structures that are the most likely to be associated with a strong ageastrophic circulation and thus
255 with biomass enhancements. A counter-exemple to our finding was presented by Tzortzis et al. (2021), who investigated the biological effect of less energetic fronts in the Mediterranean sea and found that they were mostly boundaries between distinct phytoplankton taxa.

https://doi.org/10.5194/egusphere-2023-471
Preprint. Discussion started: 27 March 2023

The detected biological enhancements over CCE-LTER fronts was made possible by the high across-front resolution of the sampling. Indeed, horizontal spacing between two adjacent stations along the CCE-LTER transects resolved cross-frontal patchiness, with only the coarsest transect (F2, resolution of 8 km, Fig. 6c) at the limit. Our results clearly showed that biomass peaks are thinner than the front and could have easily be missed with a coarser sampling. However, it is also possible that structures at an even finer cross-frontal scale exist : for instance, Chekalyuk et al. (2012) showed the presence of a patch of *Synechococcus* only 100m wide in the A-front using continuous shipboard measurement that was missed in the CTD transect.

One limit of the CCE-LTER data set is that HPLC samples were only analyzed at the surface for most of fronts, which did not allow the detection of peaks when they were in the subsurface. Nevertheless Chl-a fluorescence measurements, which were conducted continuously during each CTD profile, provided useful and complementary information on the vertical structure of phytoplankton despite their low taxonomic resolution. For instance at front F2, there was no visible HPLC-surface diatom peak but there was a peak in the vertically integrated Chl-a fluorescence (right panel in fig. 6), suggesting that the biomass enhancement was likely at subsurface. In other cases, we noted that some of the phytoplankton peaks detected by surface measurements were horizontally shifted from the vertically integrated values of both zooplankton and Chl-a fluorescence (e.g. fronts E1 and F3). Indeed, vertical profiles of Chl-a fluorescence revealed that chlorophyll layers were tilted (Supp. fig. A5), which can explain both the horizontal shift and the wider scale of the vertically integrated peaks. Tilted layers are commonly found in frontal structures and are indicative of the vertical ageostrophic circulation generated during frontogenesis (de Verneil et al., 2019). In addition, a finer vertical resolution than achieved in CTD transects might be necessary to fully resolve the vertical structures. Indeed, the use of the MVP at the E-front revealed the presence of very fine vertical layers (1-10m) in the chlorophyll-a and salinity distributions (de Verneil et al., 2019) that were only partially resolved with the Niskin bottle data, which were collected with a vertical resolution of 10-20m). Moreover, the use of an in-situ imaging system in towed instruments similarly revealed heterogeneities in the zooplankton distribution at scales of a few meters (Ashjian et al., 2001).

This dataset provides a snapshot view of the planktonic ecosystem but cannot capture their time evolution. Thus, our estimates of frontal enhancement might not be representative of the mean amplification over a longer period of time. Spatio-temporal variability at fronts may result from three factors : first, frontal communities may not at equilibrium because the nutrient supply is intermittent. For example, the C3-front does not have a biomass enhancement despite the presence of a very intense density gradient. One explanation for this paradoxical situation is the delay between the onset of the nutrient injection and the accumulation of phytoplankton and zooplankton biomass. If the transect had been conducted a few weeks or maybe even a few days later, biological enhancements might have been detected.

Second, fronts are constantly being displaced by the horizontal circulation (which is particularly intense in the CCE) and their location can change quickly and unpredictably. It is thus difficult to follow the evolution of a front over a few weeks. The 2012 cruise attempted to do this by performing two transects (E1 and E2) at the same coordinates 2 weeks apart. However, the physical seascape shifted in the interval because of the unexpected arrival of a coastal filament, which resulted in two different structures being sampled in the two transects (Supp. Fig. A3 and videos). This example highlights the need to follow in real-time the evolution of water masses before choosing the location of a transect. This requires real-time Lagragian analysis of satellite data (e.g., using the SPASSO software as in Tzortzis et al. (2021)).

https://doi.org/10.5194/egusphere-2023-471
Preprint. Discussion started: 27 March 2023

Third, water is advected quickly along the fronts : frontal jets often have velocities of $0.5\mathrm{m/s}$, i.e., about 50 $\mathrm{km/day}$. The composition of a plankton community at a given transect site thus depends on the conditions upstream of the front and the history of the water masses. Specifically in the CCE, the horizontal circulation connects fronts with the coastal upwelling zone, whose intensity strongly varies over only a few days. These short upwelling pulses can generate chlorophyll patches that are then advected away from the coast by mesoscale eddies and frontal jets, and can result in along-front patchiness (Gangrade and Franks, 2023).

4.2 What does the taxonomic structure tell us about the driving processes ?

In "transition fronts", the composition of the frontal community can be explained by simple cross-frontal mixing between communities on the warm side and cold side, respectively. In contrast, the specific community encountered in "peak fronts" requires additional processes capable of selectively increasing the biomass of some groups, such as local growth, transport from a more productive region, and/or biotic interactions (Fig. 8).

We found that the enhancement of total biomass is associated with a modification of the community structure. This implies that different taxa respond in different ways to frontal dynamics. In particular, we examined the behavior of rarer taxa that are masked by the dominant groups when only the total chlorophyll or the total particle count are measured. Importantly, we found that two taxa with similar ecological roles within a trophic group can have different responses at fronts.

We found that many taxa of both phytoplankton and zooplankton are almost systematically associated with fronts. While this behavior is well-known for some of them (particularly diatoms (Franks, 1992; Claustre et al., 1994; Yoder et al., 1994; Allen et al., 2005; Ribalet et al., 2010; Carreto et al., 2016), copepods (Boucher, 1984; Thibault et al., 1994; Derisio et al., 2014) and gelatinous zooplankton (Graham et al., 2001; Luo et al., 2014)), the effect of fronts on other taxa have only been investigated very occasionally (e.g., Capitanio and Esnal (1998) for appendicularians).

The most intuitive explanation for the high abundance of these groups is increased growth in response to the supply of nutrients. Most of the fronts included in this analysis are relatively stable, and the physical structures underlining them (SST or SSH gradients and FSLE ridges) are generally visible on satellite images at least a few weeks before each transect was conducted, depending on the cloud cover (supp. videos). Such timescales, in principle, are long enough to support the local growth of phytoplankton and most meso-zooplankton in response to the frontal vertical circulation. But a causal link is difficult to establish because of the large uncertainties associated with the estimation of the time elapsed since the frontal gradient intensified and with the reproduction rates of zooplankton. It should be noted that injections of nutrients at fronts should only produce an increase of the growth rates if the phytoplankton population is nutrient-deprived, which is not the case for every front (Supp. Fig. A10). Interestingly, however, the "younger" fronts (F1-F2, which can only be identified on satellite images for a few days before the transects) show less zooplankton enhancement than the other fronts. The zooplankton taxon with the fastest reproduction rate, the appendicularians, is also the one most strikingly enhanced at fronts (Fig. 5). However, we cannot rule out the possibility that peaks of both biomass and secondary production are attributable to advection along the front of a more productive water mass. The elucidation of the relative importance of these two processes requires taking into account the history of the water masses by adopting a Lagrangian perspective.

https://doi.org/10.5194/egusphere-2023-471
Preprint. Discussion started: 27 March 2023

Finally, the third process - biotic interactions - may explain some of the differential responses among plankton groups. Indeed, we found that many phytoplankton taxa other than diatoms often have lower abundances at fronts than in their surroundings. A recent modelling study offers a possible mechanism which could explain this observation : Mangolte et al. (2022) showed how two competitive processes can be intensified by the frontal conditions, resulting in lower abundances of cyanobacteria and coccolithophores : community shading (reduced growth rate because of light competition with another phytoplankton group located higher in the water column) and shared predation (increased grazing losses because of a shared predator with another group). However, it should be noted that the decrease of some of the phytoplankton groups was not shown in additional measurements made in the A-front with a different methodology (epifluorescence microscopy). The minima of prymnesiophytes and dinoflagellates HPLC-derived biomass were either much reduced or absent from the microscopy measurements (Fig. A8). One explanation is that the pigment composition of these groups was different at the front, possibly as a result of a change at the species level, and was interpreted as a lower abundance by the HPLC methodology (which relies on the assumption of a constant pigment composition). Another explanation is that the cell counts produced by the epifluorescence microscopy semi-automated system underestimated the abundance of these groups outside the front, possibly also as a result of a modification of the species assemblage at the front. Both explanations suggest that a higher level of taxonomical resolution (up to the species level, for instance provided by genomics) may be necessary to go further in our understanding of the effect of fronts on phytoplankton communities.

In the case of cyanobacteria, a shared predation mechanism involving heterotrophic bacteria as the competing prey and nano-zooplankton (heterotrophic nanoflagellates and ciliates) as the common predator was introduced by Goericke (2011) and later termed the "enhanced microbial loop" by Taylor and Landry (2018). In these studies, this mechanism was invoked to explain large scale patterns of phytoplankton community structure (for instance between productive coastal waters and oligotrophic offshore waters at scales of 100s of km); here we suggest that it could also play a role at much smaller scales (1-10 km, i.e., between productive frontal waters and an oligotrophic background). In the enhanced microbial loop framework, the elevated POC concentration (such as detritus or faecal pellets) and associated microbial activity leads to an increase of nano-flagellate predation on both heterotrophic and cyanobacteria, ultimately resulting in a decrease of the abundance of cyanobacteria. Indeed, Samo et al. (2012) showed that the growth of heterotrophic bacteria is elevated in the A-front, and attributed the absence of a similarly elevated biomass to viral lysis. We also suggest that the shared predation could be mediated by appendicularians in addition to nano-zooplankton. Appendicularians are also likely to play a particularly important role in the top-down regulation of bacteria because their extremely high growth rates allow them to react quickly to an increase in their food supply (Capitanio and Esnal, 1998). Many of the other fronts in our meta-analysis similarly have a moderate increase of bacteria and a very high increase of appendicularians; however the omission from the measurements of nano-zooplankton (heterotrophic nanoflagellates and ciliates) prevents us from drawing conclusions on the relative importance of the two trophic pathways, limiting our understanding of the biotic processes regulating plankton communities at fronts.

Thus, in the CCE-LTER fronts, the plankton community structure is likely regulated by the coupling of transport and biotic interactions, including both bottom-up (growth in response to nutrient injections) and top-down (elevated grazing pressure) processes.

https://doi.org/10.5194/egusphere-2023-471
Preprint. Discussion started: 27 March 2023

4.3 What does the spatial structure tell us about the driving processes ?

We found that there is cross-frontal patchiness at scales smaller than the front (Fig. 8): biomass peaks (2-10 km) are narrower than physical fronts (10-30 km) and they are shifted toward the cold side (more commonly) or the warm side by up to 10 km. Furthermore, the peaks of different plankton taxa can have different positions along the transect and different widths.

The fine scale cross-frontal patchiness suggests that there are processes capable of spatially decoupling the biomass of different plankton taxa, creating multiple adjacent communities rather than a single "frontal plankton community". Importantly, the spatial decoupling is affecting closely interacting taxa (such as competitors and prey/predators) that are expected to remain together in a purely bottom-up scenario.

Therefore, additional processes such as advection by currents and biotic interactions, are necessary to explain the observed patchiness. Two scenarios could explain how such different communities could be located in such proximity (Fig. 8). First, these communities could have been generated in remote locations and brought together by the converging horizontal circulation. The different taxonomic structures would be caused by the different environmental conditions (such as the date and intensity of the nutrient supply) experienced by the water masses. The analysis of water mass trajectories supports this scenario at the E-front (de Verneil et al., 2019), while a cursory examination of satellite data suggests that it is also the case in some of the other fronts in this analysis (most notably C2, supp. Fig. A2).

Second, an initially homogeneous frontal community could have evolved in different ways because of differences in the environmental conditions across the frontal gradient. These differences could involve the nutrient supply : the frontal injection of nutrients is theoretically located on the warm side because of the direction of the ageostrophic frontal circulation, and meanders of the fronts can create a geostrophic pumping of nutrients on either side (Oguz et al., 2015; Lohrenz et al., 1993). They could also be related to differences in stratification and temperature, which can influence a variety of biotic processes from the growth rates of phytoplankton to the vertical migration (DVM) of zooplankton and the prey-predator encounter rates. The patchiness can be maintained at a very fine scale (a few kilometers) as long as the timescale of these biological processes is faster than turbulent mixing.

5 Conclusions

In this study, we describe the taxonomic structure and fine scale spatial organization of plankton communities across ten fronts in the California Current Ecosystem upwelling region. The hypothesis of frontal nutrient injections explains the predominance of diatoms at fronts, but needs to be supplemented by other processes to explain the differential responses of the other plankton groups and the cross-frontal patchiness. By improving the horizontal and the taxonomic resolution, we gain a more complete view of fronts as complex structures driven by the coupling of physical and biological processes.

The understanding of the role of fronts on marine ecosystems by empirical means can be improved in two ways. Firstly, frontal communities should be sampled at appropriate horizontal, vertical, taxonomic and temporal resolution. While many instruments can achieve excellent performance at one scale, the challenge lies in simultaneously increasing all the dimensions of resolution, which can be achieved by strategically combining multiple shipboard and autonomous instruments. Secondly,

https://doi.org/10.5194/egusphere-2023-471
Preprint. Discussion started: 27 March 2023

the quantification of production and transport rates is extremely helpful in order to evaluate the role of the various processes. This can be achieved by in-situ measurement of the growth and grazing rates and the adoption of a Lagrangian perspective.

The elucidation of the structure of frontal ecosystems and of the processes driving them should then allow the development of parametrizations in order to include fronts in global climate models and fishery management models and evaluate their contributions to the cycling of matter and energy in the ocean.

Code and data availability. The original datasets are available on the CCE-LTER database (https://oceaninformatics.ucsd.edu/datazoo/catalogs/ccelter/datasets) and at the Environmental Data Initiative site (https://edirepository.org/). The code used to perform the analysis and the data in netCDF format are available at https://doi.org/10.5281/zenodo.7734963

Video supplement. Videos corresponding to the snapshots of Figs A1, A2 , A3 , and A4 extended to 3 months before and after the transects are available as supplementary material

Appendix A: Description of the structure and context of the fronts

The following sections describe the regional context of each of the four cruises and the physical structure of each transect. We present the transect CTD data (Fig. 4 and vertical distribution in Supp. Fig. A9) and we reconstitute the evolution of the frontal structures in the weeks before and after the transect date by visually examining satellite data (Supp. Figs. A1-A2-A3-A4 and videos).

A-front

In October 2008, an SST front named the "A-front" was identified and sampled in a single 25 km transect consisting of 9 stations spaced by about 3 km. The data from this transect, along with other measurements taken during the cruise, were extensively analyzed (including the physical and ecological properties of the front, from bacteria to fishes) and published in a series of papers (see Landry et al. (2012) for a summary of the results).

Transect A crossed an isolated, narrow front (the A-front), clearly marked by steep density and temperature gradients at stations 3-4-5 (forming a front about 5 km wide, Fig. 6a). It separates warm waters on the south side (stations 1-2) from colder waters on the north side (stations 6-7-8). The A-front is located just north of the California Current, which is caracterized by a subsurface minimum of salinity visible in station 1 (Supp. Fig. A9). Satellite data (SST and water age, supp. Fig. A1 and videos) show that the A-front was sharpened about 3 weeks before the transect was conducted, when the arrival of a mass of upwelled water from the north suddenly intensified the north-south temperature gradient. An anticyclonic eddy also developed on the south side of the front as the gradient intensified. In-situ velocity data and the results of numerical simulations showed that the A-front is associated with an eastward, along-front geostrophic current and a vertical cross-frontal ageostrophic circulation

https://doi.org/10.5194/egusphere-2023-471
Preprint. Discussion started: 27 March 2023

supplying nutrients to the euphotic zone (Li et al., 2012). The A-front is about 200 km long and remained nearly stationary for months after the cruise, suggesting that its ecological impacts could be significant.

C-front

In July 2011, a frontal structure was identified and named the "C-front" because it crosses the California Current. Three transects were conducted : the first transect, C1, was initiated before the precise location of the front was known from the MVP survey and was quickly aborted because it did not adequately capture the front; it is not included in the present study. C2 and C3 were then conducted, both include 10 stations over about 20 km, with a spacing of about 2 km. The distribution and biogeochemical properties of diatoms were investigated in Krause et al. (2015) and Brzezinski et al. (2015).

Transect C2 crossed a weak thermal front separating a warm-core anticyclonic eddy on the west (offshore) from colder waters on the east (inshore). The transect is relatively short compared to the width of the front, and barely samples the cold and warm sides (Supp. Fig. A9). Notably, the temperature variation, although weak, is not uniform across the front: the temperature gradient is largest at stations 3 and 8, with a step of virtually constant temperature at stations 5-6-7. Also notably, the temperature gradient is strongly compensated by the salinity, resulting in a low density gradient. The SST and SSH signature of the eddy are visible at least 3 months before and 3 months after the transect (supp. Fig. A2 and videos), suggesting that this frontal structure is relatively stable. Satellite data show the presence of a geostrophic current flowing south around the anticyclonic eddy, transporting water of coastal origin; the water age analysis shows that this water left the coast about 6 weeks before the transect.

Transect C3 crossed a very intense salinity front aligned with an extremely narrow cold filament (stations 7-8-9), delimited by two thermal fronts at the filament's boundaries (Supp. Fig. A9). The complex salinity and temperature distributions lead to some thermohaline compensation (particularly on station 7), but a clearly defined density front is visible on stations 8-9-10. The presence of clouds and the resolution of the satellite data make it difficult to identify precisely the structure sampled and the origin of the water. However, a reasonable hypothesis would be that a strong geostrophic front, driven by salinity, generated a horizontal current which advected the cold filament along the salinity front.

E-front

In August 2012, a frontal structure at the boundary between two eddies, identified in SSH images, was named the "E-front" (with E for eddy) and sampled in two transects, E1 and E2, which are both 50 km long and were conducted at the same coordinates two weeks apart. The resolution of E1 varies from 2 to 5 km, with stations more closely spaced in the center of the transect, while E2 has a constant spacing between station of 5 km. The horizontal and vertical circulation at the E-front were investigated by De Verneil and Franks (2015); de Verneil et al. (2019); Stukel et al. (2017) with a Lagrangian analysis and a model, respectively. Bednaršek and Ohman (2015) examined the distribution of shelled zooplankton across the front.

Transect E1 crossed a front in temperature and density between a warm anticyclonic eddy on the west (offshore) and a cold cyclonic eddy on the east (inshore). The frontal region is a wide area of steep temperature and density gradients (stations 5 to 10, with a width of about 20 km) separating warm, fresh water (stations 1-4) from cold, saltier water (stations 11-13). As noted

https://doi.org/10.5194/egusphere-2023-471
Preprint. Discussion started: 27 March 2023

by previous studies, the geostrophic jet flowing south along the front is the convergence of water masses of different origins, some from upwelling sites to the east and north of the transect zone, and some from offshore (de Verneil et al. (2019); Gangrade & Franks, in review). The water age analysis also shows water parcels of different origins in the frontal region, including some that left the coast 6 weeks and some 10 weeks before the transect. This front is a relatively stable structure, the 2 eddies remain mostly stationary for about 2 months before and 1 month after the transects.

Despite being conducted only two weeks later at the same coordinates, the E2 transect crossed a different frontal structure because the two eddies and the E1 front were pushed offshore by the arrival of a coastal filament transporting recently upwelled water. This coastal filament (which is approximately 30 km wide) originated at an upwelling site east of the transect about 3 weeks earlier (Fig A3 and supplementary videos) and was transported anti-clockwise around a cyclonic eddy located east of the transect. The cold filament is aligned with a very intense salinity front, which leads to some thermohaline compensation on station 3. However two separate density fronts are visible, mainly driven by the two thermal fronts which separate the cold filament waters (stations 4-5-6) from the warmer waters outside of it (9-10 and 1-2): front E2a (stations 6-7-8) is the western edge of the filament and front E2b (station 3) correspond to its eastern edge. At the time of the transect, 3 water masses of different ages were present in the frontal region : young filament water (20 days old), older filament water (40 days old) and very old water trapped inside the eddy (3 months old). A likely scenario for the formation of this structure is the advection of recently upwelled water (the "young filament) along the geostrophic salinity front.

F-front

In June 2017, a coastal filament (the Morro Bay filament) transporting cold, recently upwelled and productive water offshore (Zaba et al., 2021) was identified and 3 transects were conducted across it. The fronts separating the cold filament water and the warmer water around it are collectively named the F-fronts. F1 is the closest to the shore, followed by F2 (10 days later) and then F3 (5 days later). F1 and F3 have a high resolution, similar to the previous cruises, while F2 is much longer and has a lower resolution of about 8 km.

Transect F1 crossed the entire filament and contains two fronts which correspond to the two edges of the filament : front F1a on the southern edge (stations 2-3) and front F1b (stations 9-10) on the northern edge. For both fronts, the cold side is the core of the filament (stations 4-8) and the warm side is outside the filament (stations 1 and 11). There is a complex thermohaline structure associated with the filament and the fronts, with steps in temperature that do not translate to the density structure, such that the frontal stations are better seen on the density structure.

Transect F2 also crossed the entire coastal filament, however the front forming the southern edge of the filament (around stations 5-6) is weaker and compensated in density and was not included in the analysis. Stations 1-5 are part of an older filament which left the coast about 40 days before the transect (in contrast to the main filament, which left the coast less than 20 days before the transect). The F2 front thus corresponds to the northern edge of the main filament and is well defined by the elevated temperature and density gradients at stations 9-10-11. The warm side is outside the filament (station 11) and the cold side is inside (stations 7-8).

https://doi.org/10.5194/egusphere-2023-471
Preprint. Discussion started: 27 March 2023

Transect F3 crossed a wide region of strong temperature and density gradient (stations 5-11, 30 km width), corresponding to a transition between warm offshore waters (stations 1-5) and colder waters (station 11). These colder waters left the coast east of the transect 3 weeks before the F3 transect was conducted (Fig. A4). Similarly to the C2 and F1a fronts, the temperature along F3 varies in steps, with stretches of flat gradient within the wide frontal region (in stations 7-8-9). The FSLE and water age analysis suggest that this frontal region contains a narrow stirring filament transporting older coastal water (6 weeks) in a trajectory parallel to the main coastal filament. The secondary filament was initially flowing southward but was pushed offshore by the main filament and is curved around it on the west side at the time of the F3 transect. The water of the secondary filament is older than the main filament (6 weeks vs 3 weeks).

Summary

In summary, this examination has revealed that all transects crossed temperature and/or density gradients (indicating the presence of a "front"), whose width varied between 5 and 30 km. In some fronts, the density varies in a single step (A, C3, E1, E2, F2). In the others (C2, F1, F3), the density varies in multiple steps, indicating the presence of structures at a scale smaller than the width of the front. Satellite data suggest that many of the fronts are associated with strong currents that are advecting filaments along the fronts. In some cases, multiple filaments are converging in the frontal zone.

https://doi.org/10.5194/egusphere-2023-471
Preprint. Discussion started: 27 March 2023

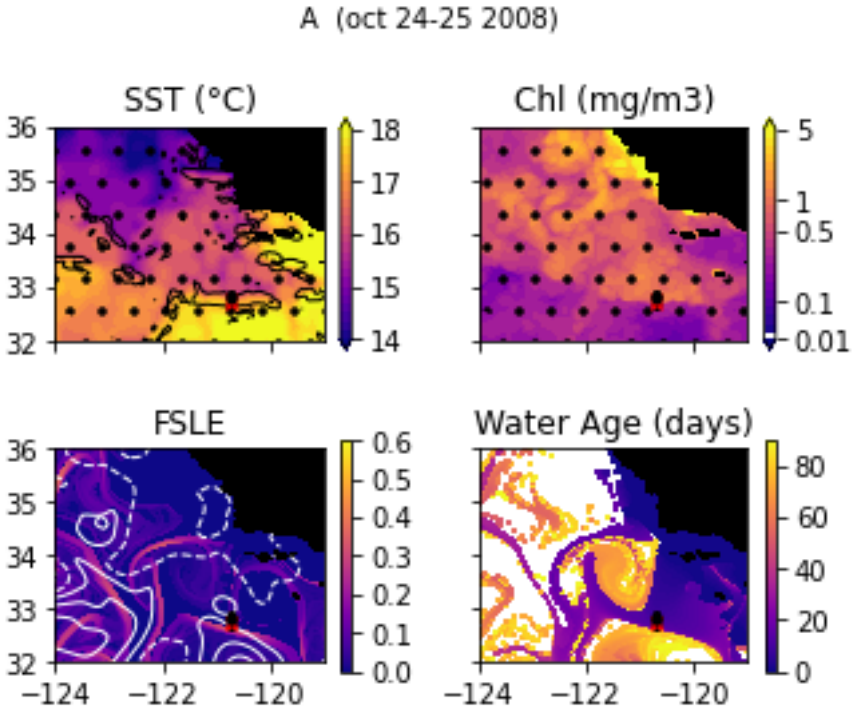

Figure A1. Snapshots of satellite-derived data at the time of transect A : SST (black lines indicate SST fronts (HI>10)), chlorophyll, FSLE (with SSH in white contours at 0,0.05,0.1,0.15,0.2,0.25,0.3 m above geoid; dashed lines indicate cyclonic eddies and solid lines anticyclonic eddies) and water age (in days since the water parcel left the coast). The hatches indicate the presence of clouds, where the fields are smoothed by the interpolation (resulting in weaker gradients).

https://doi.org/10.5194/egusphere-2023-471
Preprint. Discussion started: 27 March 2023

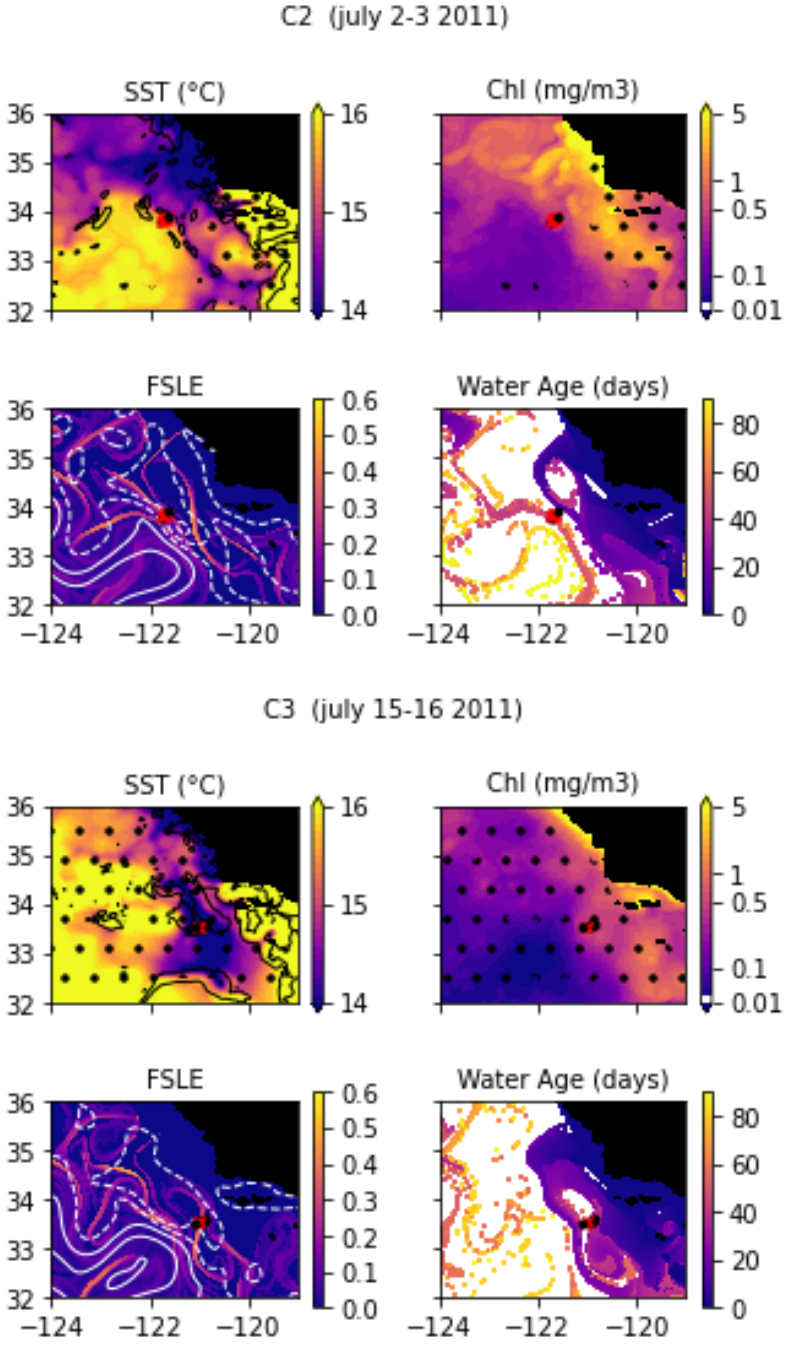

Figure A2. Snapshots of satellite-derived data at the time of transects C2 and C3 : SST (black lines indicate SST fronts (HI>10)), chlorophyll, FSLE (with SSH in white contours at 0,0.05,0.1,0.15,0.2,0.25,0.3 m above geoid; dashed lines indicate cyclonic eddies and solid lines anticyclonic eddies) and water age (in days since the water parcel left the coast). The hatches indicate the presence of clouds, where the fields are smoothed by the interpolation (resulting in weaker gradients).

https://doi.org/10.5194/egusphere-2023-471
Preprint. Discussion started: 27 March 2023

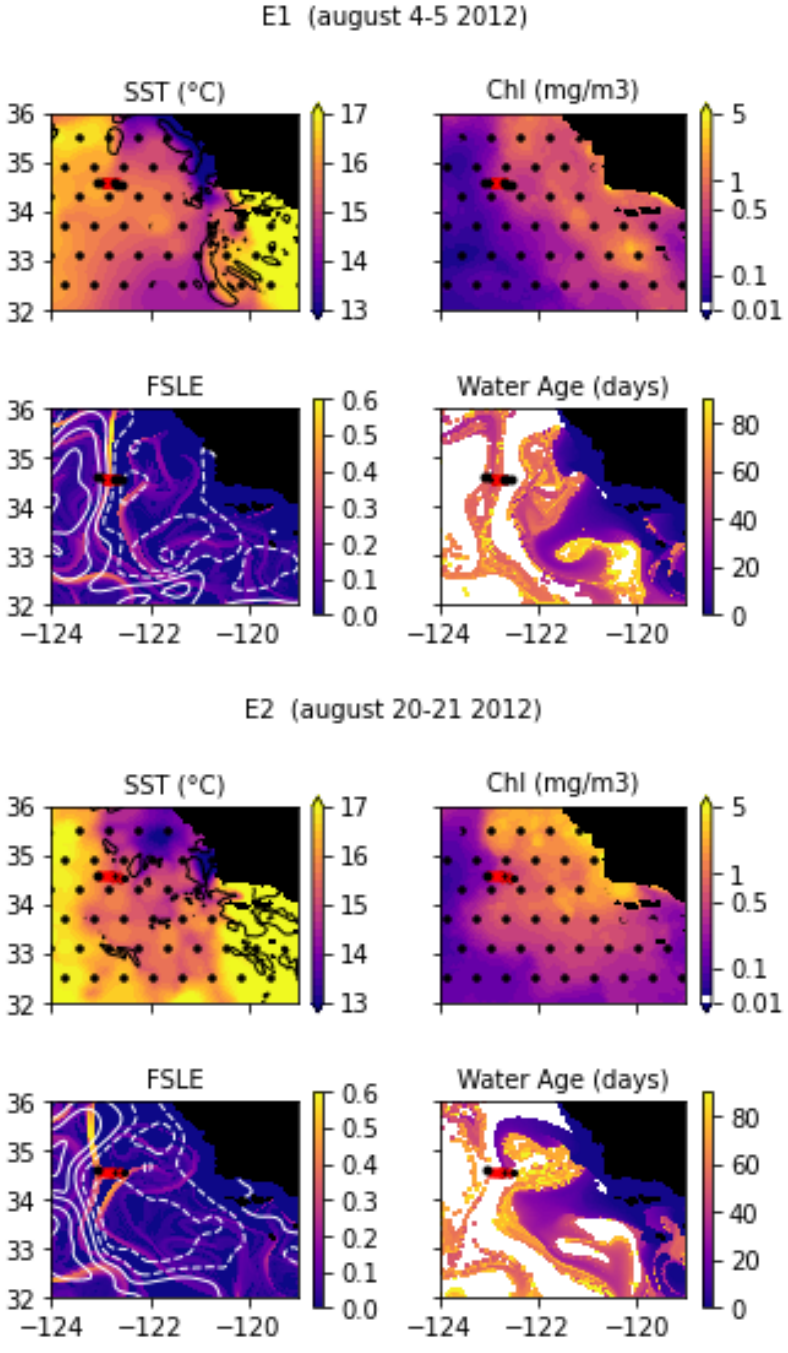

Figure A3. Snapshots of satellite-derived data at the time of transects E1 and E2 : SST (black lines indicate SST fronts (HI>10)), chlorophyll, FSLE (with SSH in white contours at 0,0.05,0.1,0.15,0.2,0.25,0.3 m above geoid; dashed lines indicate cyclonic eddies and solid lines anticyclonic eddies) and water age (in days since the water parcel left the coast). The hatches indicate the presence of clouds, where the fields are smoothed by the interpolation (resulting in weaker gradients).

https://doi.org/10.5194/egusphere-2023-471
Preprint. Discussion started: 27 March 2023

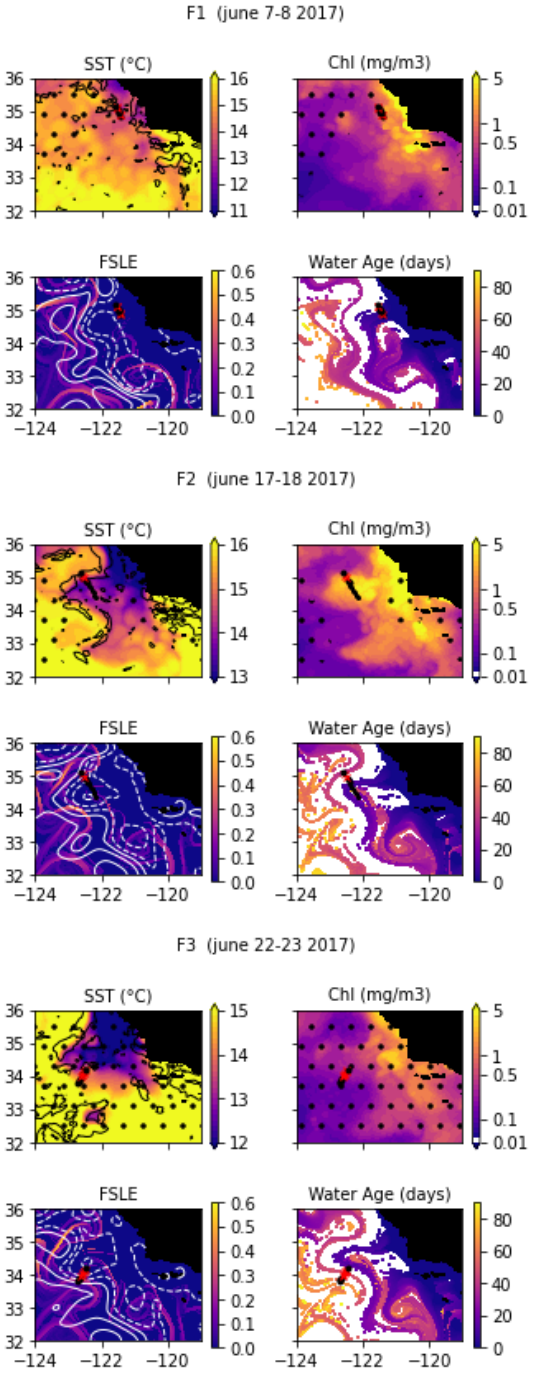

Figure A4. Snapshots of satellite-derived data at the time of transects F1, F2 and F3 : SST (black lines indicate SST fronts (HI>10)), chlorophyll, FSLE (with SSH in white contours at 0,0.05,0.1,0.15,0.2,0.25,0.3 m above geoid; dashed lines indicate cyclonic eddies and solid lines anticyclonic eddies) and water age (in days since the water parcel left the coast). The hatches indicate the presence of clouds, where the fields are smoothed by the interpolation (resulting in weaker gradients).

https://doi.org/10.5194/egusphere-2023-471
Preprint. Discussion started: 27 March 2023

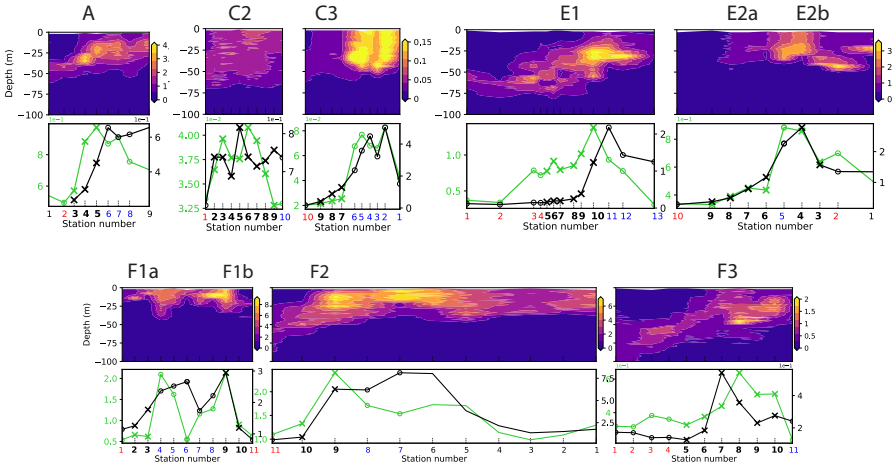

Figure A5. Top row : vertical sections of fluorescence. Bottom row : vertically integrated fluorescence (0-100 m) and HPLC-derived surface chl-a. Front stations are indicated by crosses and the background stations by circles; the numbers of the frontal stations are written in bold and the warm and cold sides in red and blue.

https://doi.org/10.5194/egusphere-2023-471
Preprint. Discussion started: 27 March 2023

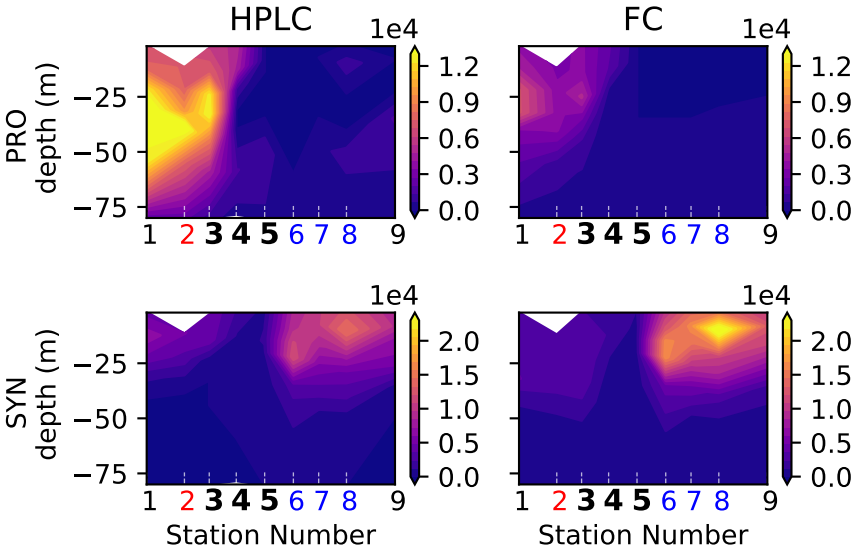

Figure A6. Biomass of cyanobacteria (*Prochlorococcus* on the left, *Synechococcus* on the right in the A-front transect measured by two different instruments : HPLC (top row) and Flow Cytometry (bottom row). The numbers of the frontal stations are written in bold and the warm and cold sides in red and blue.

https://doi.org/10.5194/egusphere-2023-471
Preprint. Discussion started: 27 March 2023

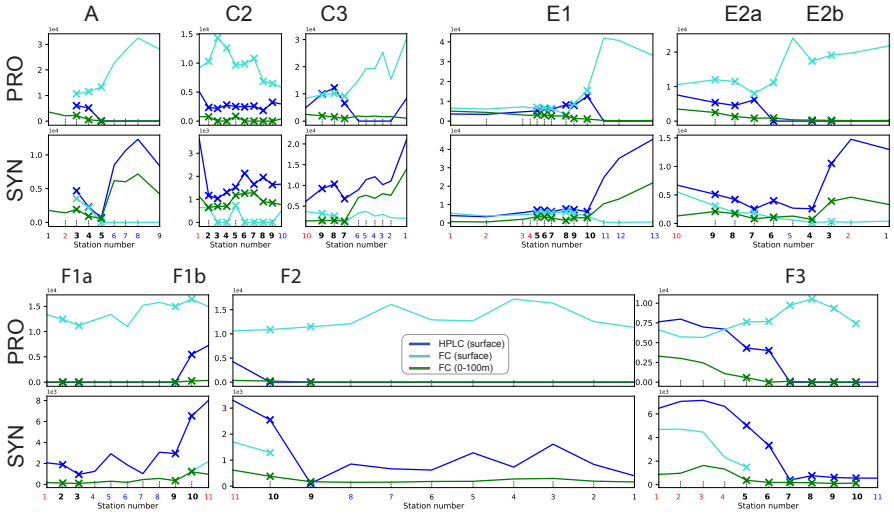

Figure A7. Depth-integrated and surface biomass ($\mu g/m^3$) of cyanobacteria (top row : *Prochlorococcus*; bottom row : *Synecococcus*) , measured by HPLC and Flow Cytometry (FC). Front stations are indicated by crosses and the background stations by circles; the numbers of the frontal stations are written in bold and the warm and cold sides in red and blue.

https://doi.org/10.5194/egusphere-2023-471
Preprint. Discussion started: 27 March 2023

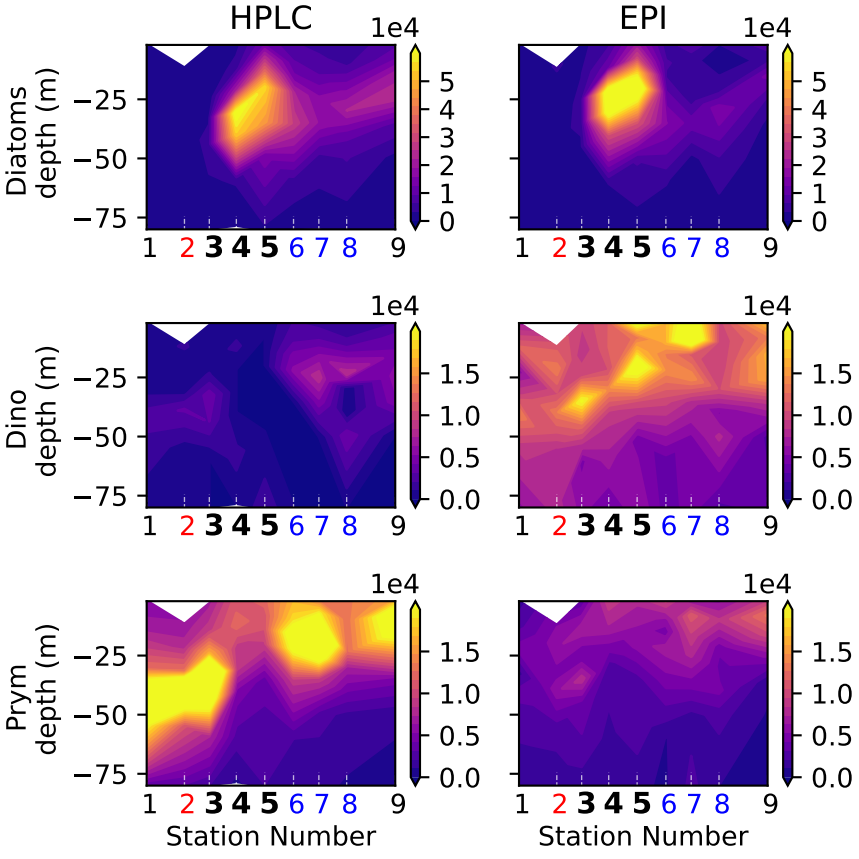

Figure A8. Biomass of eukaryotic phytoplankton (Diatoms, Dinoflagellates and Prymnesiophytes) determined by HPLC (this study) and Epifluorescence microscopy (from Taylor et al. (2012))

https://doi.org/10.5194/egusphere-2023-471
Preprint. Discussion started: 27 March 2023

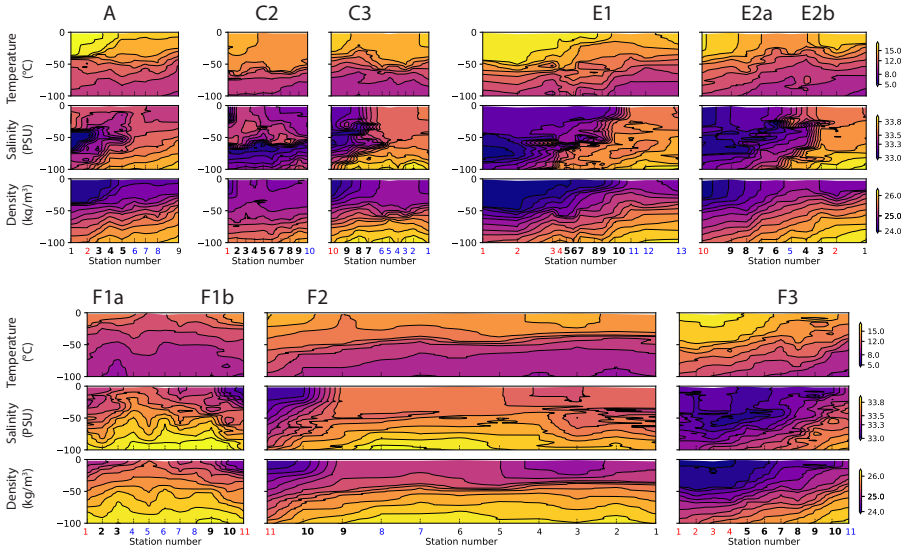

Figure A9. Vertical sections of temperature (top row), salinity (middle row) and density (bottom row) in the eight transects. Note that the colorscales are identical for all the transects. At the bottom of the plots, the numbers of the frontal stations are written in bold and the warm and cold sides in red and blue.

https://doi.org/10.5194/egusphere-2023-471
Preprint. Discussion started: 27 March 2023

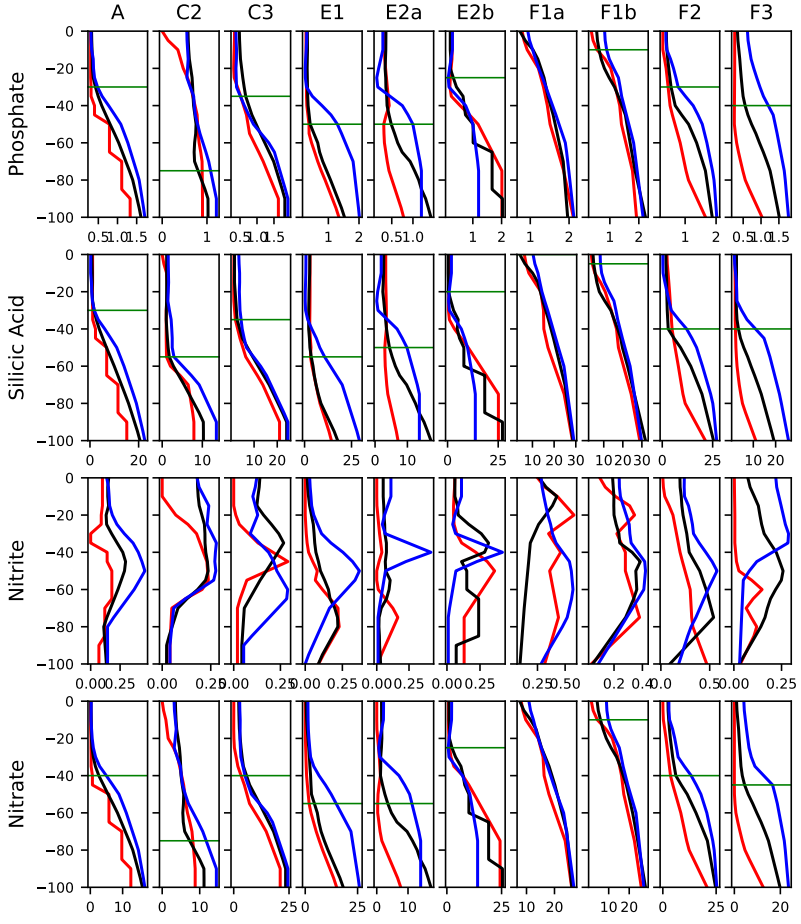

Figure A10. Vertical profiles of the concentration of nutrients (in $\mu mol/L$, averaged in the frontal stations (black lines) and the warm and cold background stations (red and blue lines, respectively). The horizontal bars shows the depth of the nutricline in the fronts.

https://doi.org/10.5194/egusphere-2023-471
Preprint. Discussion started: 27 March 2023

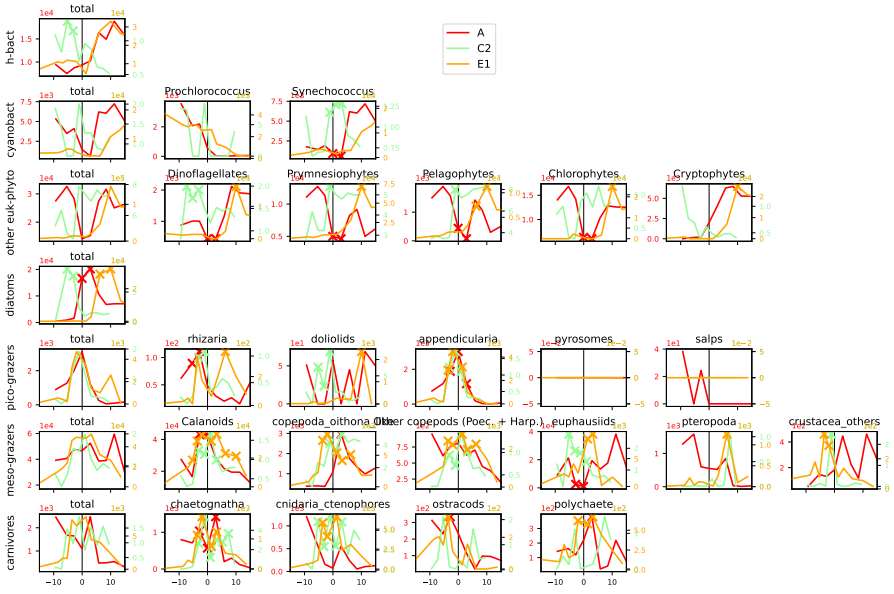

Figure A11. Distribution across fronts A, C2 and E1 of the total biomass of each trophic group (left column) and biomass of the individual taxa constituting it. The data are centered on the physical density gradient (vertical black lines), the crosses indicate the stations with a biomass peak.

https://doi.org/10.5194/egusphere-2023-471
Preprint. Discussion started: 27 March 2023

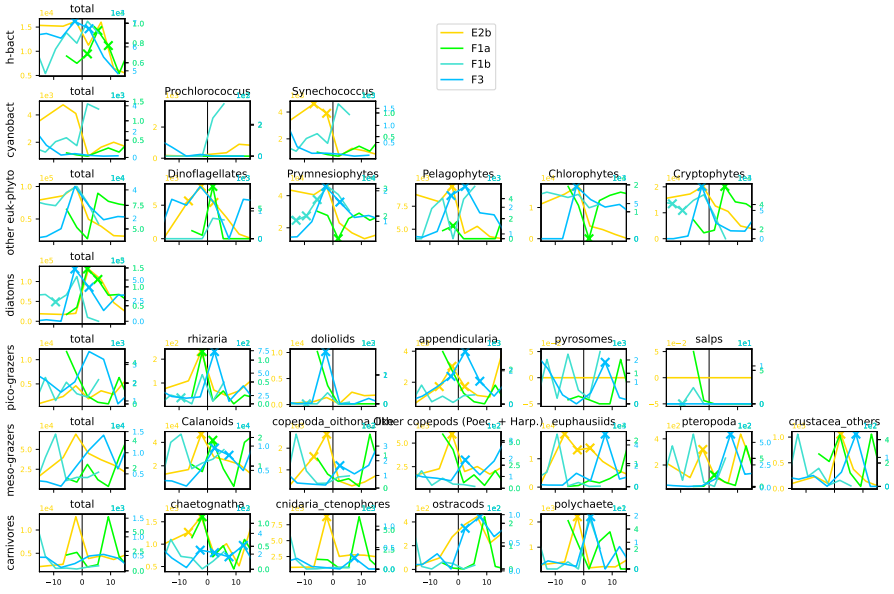

Figure A12. Distribution across fronts E2b, F1a, F1b and F3 of the total biomass of each trophic group (left column) and biomass of the individual taxa constituting it. The data are centered on the physical density gradient (vertical black lines), the crosses indicate the stations with a biomass peak.

https://doi.org/10.5194/egusphere-2023-471
Preprint. Discussion started: 27 March 2023

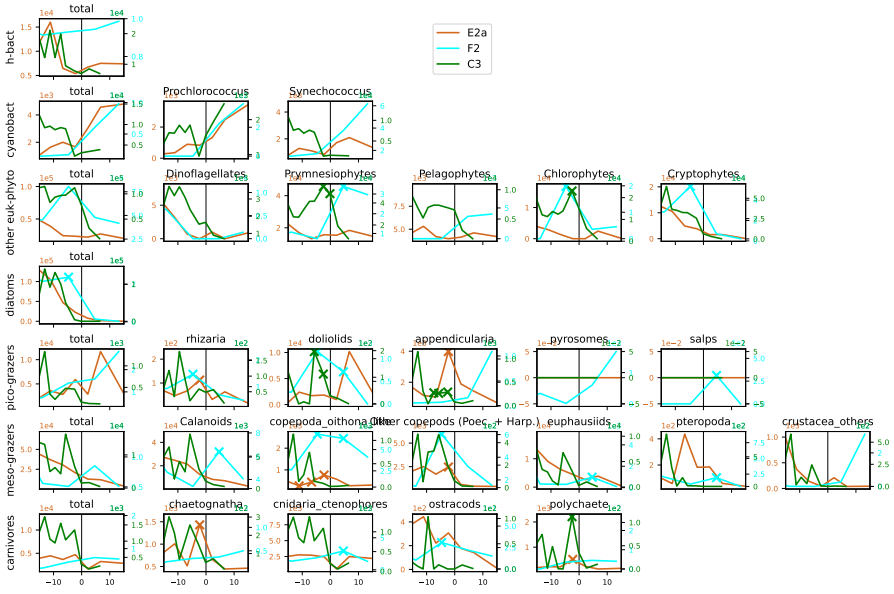

Figure A13. Distribution across fronts E2a, F2 and C3 of the total biomass of each trophic group (left column) and biomass of the individual taxa constituting it. The data are centered on the physical density gradient (vertical black lines), the crosses indicate the stations with a biomass peak.

https://doi.org/10.5194/egusphere-2023-471
Preprint. Discussion started: 27 March 2023

Author contributions. MDO provided the data. IM conducted the analysis and wrote the manuscript. All authors participated in the discussion and interpretation of the results and reviewed the manuscript.

Competing interests. The authors declare no competing interests.

Acknowledgements. IM received a PhD schlolarship from the Ecole Normale Supérieure and a visiting student Fulbright scholarship which enabled a six month stay at SIO. The project was supported with funding from CNES. Data collection was supported by the U.S. National Science Foundation in grants OCE-OCE-1026607 and OCE-1637632 to the California Current Ecosystem LTER site. We thank the crews of the ships of the P0810, P1107, P1208 and P1706 CCE-LTER Process cruises, as well as Ralph Goericke, Mike Landry and the Ohman lab for collecting and processing the samples and providing data. We thank Francesco d'Ovidio, Andrea Doglioli, Pierre Chabert, Peter Franks and Shailja Gangrade for interesting discussions that helped refine the results.

https://doi.org/10.5194/egusphere-2023-471
Preprint. Discussion started: 27 March 2023

References

Allen, J. T., Brown, L., Sanders, R., Moore, C. M., Mustard, A., Fielding, S., Lucas, M., Rixen, M., Savidge, G., Henson, S., and Mayor, D.: Diatom carbon export enhanced by silicate upwelling in the northeast Atlantic, Nature, 437, 728–732, https://doi.org/10.1038/nature03948, 2005.

Ashjian, C. J., Davis, C. S., Gallager, S. M., and Alatalo, P.: Distribution of plankton, particles, and hydrographic features across Georges Bank described using the Video Plankton Recorder, Deep. Res. Part II Top. Stud. Oceanogr., 48, 245–282, https://doi.org/10.1016/S0967-0645(00)00121-1, 2001.

Bednaršek, N. and Ohman, M. D.: Changes in pteropod distributions and shell dissolution across a frontal system in the California Current System, Mar. Ecol. Prog. Ser., 523, 93–103, https://doi.org/10.3354/meps11199, 2015.

Belkin, I. M.: Review remote sensing of ocean fronts in marine ecology and fisheries, Remote Sens., 13, 1–22, https://doi.org/10.3390/rs13050883, 2021.

Boucher, J.: Localization of zooplankton populations in the Ligurian marine front: role of ontogenic migration, Deep Sea Res. Part A, Oceanogr. Res. Pap., 31, 469–484, https://doi.org/10.1016/0198-0149(84)90097-9, 1984.

Brzezinski, M. A., Krause, J. W., Bundy, R. M., Barbeau, K. A., Franks, P., Goericke, R., Landry, M. R., and Stukel, M. R.: Enhanced silica ballasting from iron stress sustains carbon export in a frontal zone within the California Current, J. Geophys. Res. Ocean., 120, 4654–4669, https://doi.org/10.1002/2015JC010829, 2015.

Capitanio, F. L. and Esnal, G. B.: Vertical distribution of maturity stages of Oikopleura dioica (tunicata, appendicularia) in the frontal system off Valdes Peninsula, Argentina, Bull. Mar. Sci., 63, 531–539, http://hdl.handle.net/20.500.12110/paper{_}00074977{_}v63{_}n3{_}p531{_}Capitanio, 1998.

Carreto, J. I., Montoya, N. G., Carignan, M. O., Akselman, R., Acha, E. M., and Derisio, C.: Environmental and biological factors controlling the spring phytoplankton bloom at the Patagonian shelf-break front - Degraded fucoxanthin pigments and the importance of microzooplankton grazing, Prog. Oceanogr., 146, 1–21, https://doi.org/10.1016/j.pocean.2016.05.002, 2016.

Chabert, P., D'Ovidio, F., Echevin, V., Stukel, M. R., and Ohman, M. D.: Cross-Shore Flow and Implications for Carbon Export in the California Current Ecosystem: A Lagrangian Analysis, J. Geophys. Res. Ocean., 126, 1–14, https://doi.org/10.1029/2020JC016611, 2021.

Chekalyuk, A. M., Landry, M. R., Goericke, R., Taylor, A. G., and Hafez, M. A.: Laser fluorescence analysis of phytoplankton across a frontal zone in the California Current ecosystem, J. Plankton Res., 34, 761–777, https://doi.org/10.1093/plankt/fbs034, 2012.

Chelton, D. B., Gaube, P., Schlax, M. G., Early, J. J., and Samelson, R. M.: The influence of nonlinear mesoscale eddies on near-surface oceanic chlorophyll, Science (80-.)., 334, 328–332, https://doi.org/10.1126/science.1208897, 2011.

Claustre, H., Kerherve, P., Marty, J. C., Prieur, L., Videau, C., and Hecq, J. H.: Phytoplankton dynamics associated with a geostrophic front: Ecological and biogeochemical implications, J.Mar.Res., 52, 711–742, https://doi.org/10.1357/0022240943077000, 1994.

Clayton, S., Dutkiewicz, S., Jahn, O., and Follows, M. J.: Dispersal, eddies, and the diversity of marine phytoplankton, Limnol. Oceanogr. Fluids Environ., 3, 182–197, https://doi.org/10.1215/21573689-2373515, 2013.

Clayton, S., Nagai, T., and Follows, M. J.: Fine scale phytoplankton community structure across the Kuroshio Front, J. Plankton Res., 36, 1017–1030, https://doi.org/10.1093/plankt/fbu020, 2014.

Clayton, S., Lin, Y. C., Follows, M. J., and Worden, A. Z.: Co-existence of distinct Ostreococcus ecotypes at an oceanic front, Limnol. Oceanogr., 62, 75–88, https://doi.org/10.1002/lno.10373, 2017.

https://doi.org/10.5194/egusphere-2023-471
Preprint. Discussion started: 27 March 2023

De Verneil, A. and Franks, P. J.: A pseudo-Lagrangian method for remapping ocean biogeochemical tracer data: Calculation of net Chl-a growth rates, J. Geophys. Res. Ocean., 120, 4962–4979, https://doi.org/10.1002/2015JC010898, 2015.

de Verneil, A., Franks, P. J., and Ohman, M. D.: Frontogenesis and the Creation of Fine-Scale Vertical Phytoplankton Structure, J. Geophys. Res. Ocean., 124, 1509–1523, https://doi.org/10.1029/2018JC014645, 2019.

Derisio, C., Alemany, D., Acha, E. M., and Mianzan, H.: Influence of a tidal front on zooplankton abundance, assemblages and life histories in Península Valdés, Argentina, J. Mar. Syst., 139, 475–482, https://doi.org/10.1016/j.jmarsys.2014.08.019, 2014.

Franks, P. J.: Sink or swim: Accumulation of biomass at fronts, Mar. Ecol. Prog. Ser., 82, 1–12, https://doi.org/10.3354/meps082001, 1992.

Gangrade, S. and Franks, P. J.: Phytoplankton patches at oceanic fronts are linked to coastal upwelling pulses: Observations and implications in the California Current System, J. Geophys. Res. Ocean., pp. 1–27, https://doi.org/10.1029/2022JC019095, 2023.

Garrison, D. L., Gowing, M. M., Hughes, M. P., Campbell, L., Caron, D. A., Dennett, M. R., Shalapyonok, A., Olson, R. J., Landry, M. R., Brown, S. L., Liu, H. B., Azam, F., Steward, G. F., Ducklow, H. W., and Smith, D. C.: Microbial food web structure in the Arabian Sea: A US JGOFS study, Deep. Res. Part II Top. Stud. Oceanogr., 47, 1387–1422, https://doi.org/10.1016/S0967-0645(99)00148-4, 2000.

Goericke, R.: The structure of marine phytoplankton communities- patterns, rules and mechanisms, Calif. Coop. Ocean. Fish. Investig. Reports, 52, 182–197, 2011.

Goericke, R. and Montoya, J. P.: Estimating the contribution of microalgal taxa to chlorophyll a in the field - Variations of pigment ratios under nutrient- and light-limited growth, Mar. Ecol. Prog. Ser., 169, 97–112, https://doi.org/10.3354/meps169097, 1998.

Gorsky, G., Ohman, M. D., Picheral, M., Gasparini, S., Stemmann, L., Romagnan, J. B., Cawood, A., Pesant, S., García-Comas, C., and Prejger, F.: Digital zooplankton image analysis using the ZooScan integrated system, J. Plankton Res., 32, 285–303, https://doi.org/10.1093/plankt/fbp124, 2010.

Graham, W. M., Pagès, F., and Hamner, W. M.: A physical context for gelatinous zooplankton aggregations: A review, Hydrobiologia, 451, 199–212, https://doi.org/10.1023/A:1011876004427, 2001.

Haberlin, D., Raine, R., McAllen, R., and Doyle, T. K.: Distinct gelatinous zooplankton communities across a dynamic shelf sea, Limnol. Oceanogr., 64, 1802–1818, https://doi.org/10.1002/lno.11152, 2019.

Haëck, C., Lévy, M., Mangolte, I., and Bopp, L.: Satellite data reveal earlier and stronger phytoplankton blooms over fronts in the Gulf Stream region, pp. 1–27, https://www.researchgate.net/publication/366922714{_}Satellite{_}data{_}reveal{_}earlier{_}and{_}stronger{_}phytoplankton{_}blooms{_}over{_}fronts{_}in{_}the{_}Gulf{_}Stream{_2023.

Klein, P. and Lapeyre, G.: The oceanic vertical pump induced by mesoscale and submesoscale turbulence, Ann. Rev. Mar. Sci., 1, 351–375, https://doi.org/10.1146/annurev.marine.010908.163704, 2009.

Krause, J. W., Brzezinski, M. A., Goericke, R., Landry, M. R., Ohman, M. D., Stukel, M. R., and Taylor, A. G.: Variability in diatom contributions to biomass, organic matter production and export across a frontal gradient in the California Current Ecosystem, J. Geophys. Res. Ocean., 120, 1032–1047, https://doi.org/10.1002/2014JC010472, 2015.

Landry, M. R., Ohman, M. D., Goericke, R., Stukel, M. R., Barbeau, K. A., Bundy, R., and Kahru, M.: Pelagic community responses to a deep-water front in the California Current Ecosystem: Overview of the A-Front Study, J. Plankton Res., 34, 739–748, https://doi.org/10.1093/plankt/fbs025, 2012.

Lavaniegos, B. E. and Ohman, M. D.: Coherence of long-term variations of zooplankton in two sectors of the California Current System, Prog. Oceanogr., 75, 42–69, https://doi.org/10.1016/j.pocean.2007.07.002, 2007.

https://doi.org/10.5194/egusphere-2023-471
Preprint. Discussion started: 27 March 2023

Lévy, M., Ferrari, R., Franks, P. J., Martin, A. P., and Rivière, P.: Bringing physics to life at the submesoscale, Geophys. Res. Lett., 39, https://doi.org/10.1029/2012GL052756, 2012.

Lévy, M., Jahn, O., Dutkiewicz, S., and Follows, M. J.: Phytoplankton diversity and community structure affected by oceanic dispersal and mesoscale turbulence, Limnol. Oceanogr. Fluids Environ., 4, 67–84, https://doi.org/10.1215/21573689-2768549, 2014.

Lévy, M., Jahn, O., Dutkiewicz, S., Follows, M. J., and D'Ovidio, F.: The dynamical landscape of marine phytoplankton diversity, J. R. Soc. Interface, 12, 20150 481, https://doi.org/10.1098/rsif.2015.0481, 2015.

Lévy, M., Franks, P. J., and Smith, K. S.: The role of submesoscale currents in structuring marine ecosystems, Nat. Commun., 9, 4758, https://doi.org/10.1038/s41467-018-07059-3, 2018.

Li, Q. P., Franks, P. J., Landry, M. R., Goericke, R., and Taylor, A. G.: Modeling phytoplankton growth rates and chlorophyll to carbon ratios in California coastal and pelagic ecosystems, J. Geophys. Res. Biogeosciences, 115, 1–12, https://doi.org/10.1029/2009JG001111, 2010.

Li, Q. P., Franks, P. J., Ohman, M. D., and Landry, M. R.: Enhanced nitrate fluxes and biological processes at a frontal zone in the southern California current system, J. Plankton Res., 34, 790–801, https://doi.org/10.1093/plankt/fbs006, 2012.

Liu, X. and Levine, N. M.: Enhancement of phytoplankton chlorophyll by submesoscale frontal dynamics in the North Pacific Subtropical Gyre, Geophys. Res. Lett., 43, 1651–1659, https://doi.org/10.1002/2015GL066996, 2016.

Lohrenz, S. E., Cullen, J. J., Phinney, D. A., Olson, D. B., and Yentsch, C. S.: Distributions of pigments and primary production in a Gulf Stream meander, J. Geophys. Res., 98, 14 545–14 560, https://doi.org/10.1029/93jc00678, 1993.

Luo, J. Y., Grassian, B., Tang, D., Irisson, J. O., Greer, A. T., Guigand, C. M., McClatchie, S., and Cowen, R. K.: Environmental drivers of the fine-scale distribution of a gelatinous zooplankton community across a mesoscale front, Mar. Ecol. Prog. Ser., 510, 129–149, https://doi.org/10.3354/meps10908, 2014.

Mahadevan, A.: The Impact of Submesoscale Physics on Primary Productivity of Plankton, Ann. Rev. Mar. Sci., 8, 161–184, https://doi.org/10.1146/annurev-marine-010814-015912, 2016.

Mangolte, I., Lévy, M., Dutkiewicz, S., Clayton, S., and Jahn, O.: Plankton community response to fronts: winners and losers, J. Plankton Res., 44, 241–258, https://doi.org/10.1093/plankt/fbac010, 2022.

Mauzole, Y. L., Torres, H. S., and Fu, L. L.: Patterns and Dynamics of SST Fronts in the California Current System, J. Geophys. Res. Ocean., 125, https://doi.org/10.1029/2019JC015499, 2020.

Mousing, E. A., Richardson, K., Bendtsen, J., Cetinić, I., and Perry, M. J.: Evidence of small-scale spatial structuring of phytoplankton alpha- and beta-diversity in the open ocean, J. Ecol., 104, 1682–1695, https://doi.org/10.1111/1365-2745.12634, 2016.

Oguz, T., Macias, D., and Tintore, J.: Ageostrophic frontal processes controlling phytoplankton production in the Catalano-Balearic Sea (Western Mediterranean), PLoS One, 10, e0129 045, https://doi.org/10.1371/journal.pone.0129045, 2015.

Ohman, M. D., Powell, J. R., Picheral, M., and Jensen, D. W.: Mesozooplankton and particulate matter responses to a deep-water frontal system in the southern California Current System, J. Plankton Res., 34, 815–827, https://doi.org/10.1093/plankt/fbs028, 2012.

Ohman, M. D., Barbeau, K., Franks, P. J., Goericke, R., Landry, M. R., and Miller, A. J.: Ecological transitions in a coastal upwelling ecosystem, Oceanography, 26, 210–219, https://doi.org/10.5670/oceanog.2013.65, 2013.

Powell, J. R. and Ohman, M. D.: Changes in zooplankton habitat, behavior, and acoustic scattering characteristics across glider-resolved fronts in the Southern California Current System, Prog. Oceanogr., 134, 77–92, https://doi.org/10.1016/j.pocean.2014.12.011, 2015.

Prants, S. V.: Marine life at Lagrangian fronts, Prog. Oceanogr., 204, https://doi.org/10.1016/j.pocean.2022.102790, 2022.

https://doi.org/10.5194/egusphere-2023-471
Preprint. Discussion started: 27 March 2023

Renault, L., McWilliams, J. C., Kessouri, F., Jousse, A., Frenzel, H., Chen, R., and Deutsch, C.: Evaluation of high-resolution atmospheric and oceanic simulations of the California Current System, Prog. Oceanogr., 195, 102 564, https://doi.org/10.1016/j.pocean.2021.102564, 2021.

Ribalet, F., Marchetti, A., Hubbard, K. A., Brown, K., Durkin, C. A., Morales, R., Robert, M., Swalwell, J. E., Tortell, P. D., and Armbrust, E. V.: Unveiling a phytoplankton hotspot at a narrow boundary between coastal and offshore waters, Proc. Natl. Acad. Sci. U. S. A., 107, 16 571–16 576, https://doi.org/10.1073/pnas.1005638107, 2010.

Samo, T. J., Pedler, B. E., Ball, G. I., Pasulka, A. L., Taylor, A. G., Aluwihare, L. I., Azam, F., Goericke, R., and Landry, M. R.: Microbial distribution and activity across a water mass frontal zone in the California Current Ecosystem, J. Plankton Res., 34, 802–814, https://doi.org/10.1093/plankt/fbs048, 2012.

Stukel, M. R., Aluwihare, L. I., Barbeau, K. A., Chekalyuk, A. M., Goericke, R., Miller, A. J., Ohman, M. D., Ruacho, A., Song, H., Stephens, B. M., and Landry, M. R.: Mesoscale ocean fronts enhance carbon export due to gravitational sinking and subduction, Proc. Natl. Acad. Sci. U. S. A., 114, 1252–1257, https://doi.org/10.1073/pnas.1609435114, 2017.

Taylor, A. G. and Landry, M. R.: Phytoplankton biomass and size structure across trophic gradients in the southern California Current and adjacent ocean ecosystems, Mar. Ecol. Prog. Ser., 592, 1–17, https://doi.org/10.3354/meps12526, 2018.

Taylor, A. G., Goericke, R., Landry, M. R., Selph, K. E., Wick, D. A., and Roadman, M. J.: Sharp gradients in phytoplankton community structure across a frontal zone in the California Current Ecosystem, J. Plankton Res., 34, 778–789, https://doi.org/10.1093/plankt/fbs036, 2012.

Thibault, D., Gaudy, R., and Le Fèvre, J.: Zooplankton biomass, feeding and metabolism in a geostrophic frontal area (Almeria-Oran Front, western Mediterranean). Significance to pelagic food webs, J. Mar. Syst., 5, 297–311, https://doi.org/10.1016/0924-7963(94)90052-3, 1994.

Tzortzis, R., Doglioli, A. M., Barrillon, S., Petrenko, A. A., D'Ovidio, F., Izard, L., Thyssen, M., Pascual, A., Barceló-Llull, B., Cyr, F., Tedetti, M., Bhairy, N., Garreau, P., Dumas, F., and Gregori, G.: Impact of moderately energetic fine-scale dynamics on the phytoplankton community structure in the western Mediterranean Sea, Biogeosciences, 18, 6455–6477, https://doi.org/10.5194/bg-18-6455-2021, 2021.

Yoder, J. A., Ackleson, S. G., Barber, R. T., Flament, P., and Balch, W. M.: A line in the sea, Nature, 371, 689–692, https://doi.org/10.1038/371689a0, 1994.

Zaba, K. D., Franks, P. J., and Ohman, M. D.: The California Undercurrent as a Source of Upwelled Waters in a Coastal Filament, J. Geophys. Res. Ocean., 126, https://doi.org/10.1029/2020JC016602, 2021.